Scientific Papers of
the Department of Electrical Power Engineering of
the Wrocław University of Technology

PRESENT PROBLEMS OF POWER SYSTEM CONTROL

7

Wrocław 2016

Cover design
Piotr PIERZ

Printed in the camera ready form

Department of Electrical Power Engineering
Wrocław University of Science and Technology
Wybrzeże Wyspiańskiego 27, 50-370 Wrocław, Poland
phone: +48 71 320 35 41
www: http://www.weny.pwr.edu.pl/instytuty,52.dhtml; http://www.psc.pwr.edu.pl
e-mail: wydz.elektryczny@pwr.edu.pl

OFICYNA WYDAWNICZA POLITECHNIKI WROCŁAWSKIEJ
Wybrzeże Wyspiańskiego 27, 50-370 Wrocław
http://www.oficyna.pwr.edu.pl
e-mail: oficwyd@pwr.edu.pl
zamawianie.ksiazek@pwr.edu.pl

ISSN 2084-2201

Print and binding: beta-druk, www.betadruk.pl

CONTENTS

*signal processing, digital filter,
magnitude estimator, high speed overcurrent relay*

Mirosław ŁUKOWICZ*, Krzysztof SOLAK*,
Paweł WICHER*, Bernard WIECHA*

OPTIMIZATION OF CURRENT MAGNITUDE ESTIMATORS BASED ON MARQUARDT–LEVENBERG ALGORITHM

Digital filtering, correlation methods, time delay methods, signal differentiation are the most commonly used methods of estimating fundamental frequency orthogonal components utilized in magnitude estimators. The foundation for designing filters used in aforementioned methods are usually demanded frequency responses or signal models with their parameters to be estimated. A weak point of both approaches is frequency-domain modelling ignoring time-domain performance of the magnitude estimators. In order to fulfil the requirements of protection with the optimum speed for many different configurations, operating conditions and construction features of power systems, it is necessary to develop magnitude estimator design methods aimed at modelling with respect to high-speed response with simultaneous acceptable estimation accuracy in the steady state.

The article discusses the implementation of Levenberg–Marquardt algorithm to optimization of current magnitude estimators designed for power system protection with the focus on estimators used in instantaneous overcurrent relays. The paper presents details of optimizing algorithm, power system model used for acquisition of signal patterns and estimator performance analyzes.

1. INTRODUCTION

Current is the earliest protection quantity used in power system relaying. Modern numeric relays, equipped with digital filtering algorithms eliminating undesirable harmonics from protection signals, provide an accurate magnitude measurement of current and voltage fundamental components. However, the accuracy is sacrificed by the long duration of estimation transients after the disturbance inception.

The speed of current magnitude estimation is essential when concerned with instantaneous overcurrent relays referred to as High Speed (HS) overcurrent relays.

* Wrocław University of Science and Technology, Department of Electrical Power Engineering, Wybrzeże Wyspiańskiego 27, 50-370 Wrocław, Poland, e-mail: miroslaw.lukowicz@pwr.edu.pl, krzysztof.solak@pwr.edu.pl, pawel.wicher@pwr.edu.pl, bernard.wiecha@pwr.edu.pl

These protections are used in medium voltage networks as main protections for clearing high level current faults and in some single-end fed 110 kV power lines.

HS protection calls first of all for short time magnitude estimation transients while ensuring adequate accuracy for the assumed signal model with its disturbances such as e.g. decaying DC component and harmonics occurring in the pre- and fault states.

The article presents the method of designing orthogonal filters optimized with respect to predefined magnitude estimator algorithm they are to be used in. The optimization process is determined by the adopted objective function, the training signal model resulting from faults modelled in the single-end fed 110 kV power line, and the model of harmonic distortions occurring in these networks in Polish power system.

Digital filter design is a multistep process in which one can specify the steps essential for the project and the final properties of obtained filters. The primary step is to determine the desired properties of the filter, which usually translates to determine the desirable complex frequency response. One should then make choose of filter class and determine the criterion according to which the choice of filter coefficients will be made. The last step is the choice of the best solution method for formulated task and its solution.

The desired magnitude or phase diagrams, or both these two diagrams, are the foundation of the project in most methods of FIR filter design. Sometimes, instead of the phase diagram the desired diagram of the filter group delay is proposed.

Usually, the basis for FIR filter design is a polynomial approximation. Filter design methods can be classified with respect to the complexity as computer aided filter design methods and traditional methods. The term *traditional methods* should be understood as methods in which the filter design is carried out without the use of iterative techniques, i.e. window methods based on inverse discrete Fourier transform [1]. The traditional methods are not computationally very complex, and their applications are limited to quite specific cases with respect to approximated characteristics. When using the traditional design, additional requirements relating to the properties of the filter in time or frequency domain cannot be taken into account. Therefore, this article presents the optimal estimator design method dedicated for measuring of the fundamental frequency voltage or current component magnitude.

2. MAGNITUDE ESTIMATORS

2.1. FUNDAMENTALS

One group of magnitude estimation methods is based on orthogonal fundamental frequency components of the analyzed periodic signals. According to the Pythagoras's theorem magnitude of sine wave can be calculated from the following formula

$$I(n)=\sqrt{i_c^2(n)+i_s^2(n)} \tag{1}$$

where i_c, i_s are orthogonal components evaluated for instant n. One can obtain orthogonal components, for instance of current i, by digital filtering with coefficients $b_{c(j)}$, $b_{s(j)}$ of the pair filters according to the following formulae

$$\begin{aligned} i_c(n) &= \sum_{j=0}^{N-1} i(n-j) b_{c(j)} \\ i_s(n) &= \sum_{j=0}^{N-1} i(n-j) b_{s(j)} \end{aligned} \tag{2}$$

These filters should provide a phase shift of π/2 and the same modules of output signals for the fundamental frequency. Moreover, the proper shape of the frequency response above and below the nominal power system frequency should be ensured. Usually impact of harmonics and decaying DC offset on orthogonal components estimation should be minimized. This very well define requirements of filtering protection signals as far as magnitude estimation accuracy in the steady state is concerned, however no specification are given explicitly regarding the interaction between magnitude and phase responses and the estimation transient state desired. The most commonly used filters that meet the basic requirements listed above are orthogonal sine-cosine filters referred to as full cycle Fourier filter. These filters introduce the estimation transient state of the length that is equal to the length of filter data window. Moreover, the impact of decaying DC current components on magnitude estimation based on these filters is significant.

2.2. ESTIMATOR DESIGN BASED ON TARGET PATTERN PRESENTATION

In the proposed method, two filters orthogonal only near the system frequency, are design by minimizing of the objective function that is expressed by the following formula

$$Q(\mathbf{B}_c, \mathbf{B}_s)=\sum_{k=1}^{L}\sum_{n=1}^{K}\frac{1}{4}W(M, e(\mathbf{B}, k, n))\left(I^2(\mathbf{B}, k, n)-\hat{I}^2(k, n)\right)^2, \tag{3}$$

where

$$\mathbf{B}=[\mathbf{B}_c \quad \mathbf{B}_s]=[b_{c(0)}\ b_{c(1)} \ldots b_{c(N-1)} \quad b_{s(0)}\ b_{s(1)} \ldots b_{s(N-1)}]=[b_{(0)} \quad \ldots \quad b_{(2N-1)}] \tag{4}$$

is a parameter vector of the estimator.

For a given set of training cases, function Q takes value of the cumulative weighted squares of estimation errors. The error is defined as difference between the magnitude estimate squared and target estimate squared. An estimate error for n-th sample in k-th fault case is expressed as follows

$$e(\mathbf{B}, k, n) = I^2(\mathbf{B}, k, \mathbf{n}) - \hat{I}^2(k, n) \tag{5}$$

The square of (1) is used in (5) to avoid the computation of the partial derivative of the square root function.

The value of the objective function for a fixed set of training examples depends only on filter coefficients employed in the estimator (1-2). Sets $\mathbf{B}_c$ and $\mathbf{B}_s$ of 20 coefficients each constitute set $\mathbf{B}$ of parameters to be optimized.

The weighting function W in (3) defines the estimate transient state length (M) and steady state for $n > (M + N)$. This function eliminates from training process these data windows that are associated with sampling instants before the fault inception designated with N.

$$W(M, e(\mathbf{B}, k, n)) = \begin{cases} 1 & \text{for} \quad n \geq (M + N) \\ 1 & \text{for} \quad N + 1 \leq n < M + N \quad \text{AND} \quad e(\mathbf{B}, k, n) > 0 \\ 0 & \text{for} \quad n < N + 1 \end{cases} \tag{6}$$

Values taken by weighting function are shown in Fig. 1. The length of the transient state denoted by M is a parameter of the proposed estimator. The corresponding estimate is arbitrary for this state, but should not be greater than the magnitude at the steady state. This results in that only those moments of the transient state are used in the optimization, for which the error exceeds 1, i.e. when the overshoot of the magnitude estimate occurs.

In the proposed approach, current samples for all fault cases are normalized to provide the steady state magnitude equal to 1 as depicted in Fig. 1.

One group of iterative optimization techniques are methods based on the gradient of the objective function calculated with respect to the optimized quantities. In the proposed approach the gradient of (3) relative to the coefficients of $\mathbf{B}_c$ consists of components computed with the following formula

$$\begin{aligned} \frac{\partial Q}{\partial b_{c(l)}} &= \sum_{k=1}^{L} \sum_{n=1}^{K} W(M, e(\mathbf{B}, k, n)) e(\mathbf{B}, k, n) i_c(\mathbf{B}_c, k, n) \frac{\partial i_c(\mathbf{B}_c, k, n)}{\partial b_l} \\ &= \sum_{k=1}^{L} \sum_{n=1}^{K} W(M, e(\mathbf{B}, k, n)) e(\mathbf{B}, k, n) i_c(\mathbf{B}_c, k, n) i(k, n - l + 1) \end{aligned} \tag{7}$$

and components obtained with respect to coefficients in $\mathbf{B}_s$ with formula as follows:

$$\frac{\partial Q}{\partial b_{s(l)}}=\sum_{k=1}^{L}\sum_{n=1}^{K}W(M,e(\mathbf{B},k,n))e(\mathbf{B},k,n)i_s(\mathbf{B}_s,k,n)i(k,n-l+1) \tag{8}$$

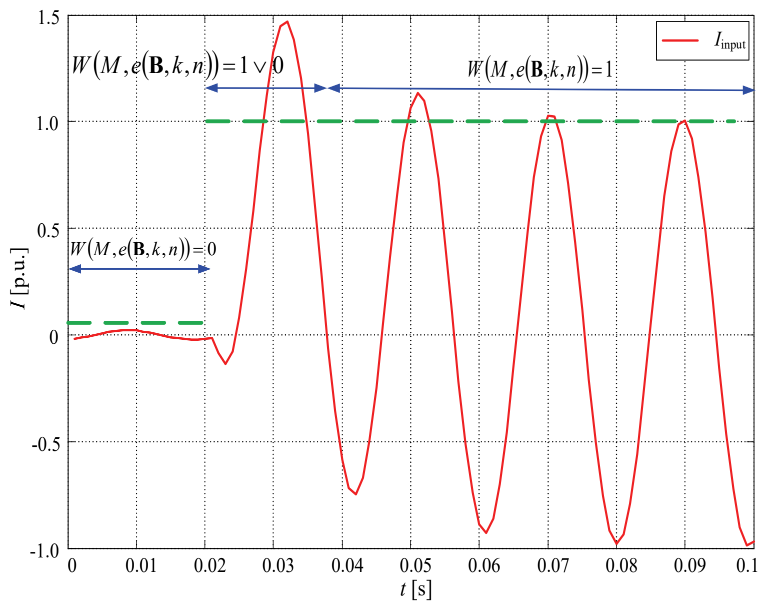

Fig. 1. Values taken by weighting function in pre fault, transient, and fault state

Since Levenberg–Marquardt method is adopted in this approach the approximation of Hessian of the following form

$$\mathbf{H}(\mathrm{Q})=\begin{bmatrix}\frac{\partial^2 Q}{\partial b_{(0)}\partial b_{(0)}} & \cdots & \frac{\partial^2 Q}{\partial b_{(0)}\partial b_{(2N-1)}}\\ \vdots & \ddots & \vdots\\ \frac{\partial^2 Q}{\partial b_{(2N-1)}\partial b_{(0)}} & \cdots & \frac{\partial^2 Q}{\partial b_{(2N-1)}\partial b_{(2N-1)}}\end{bmatrix} \tag{9}$$

has to be determined. The components of Hessian are expressed by the following formula:

$$\frac{\partial^2 Q}{\partial b_{s(m)}\partial b_{c(l)}}=\sum_{k=1}^{L}\sum_{n=1}^{K}W(M,e(\mathbf{B},k,n))i_c(\mathbf{B}_c,k,n)i_s(\mathbf{B}_s,k,n)i(k,n-l+1)i(k,n-m+1) \tag{10}$$

Updating of the coefficients in row matrix B for p-th optimizing epoch is proceeded according to the rule proposed by Levenberg and Marquardt

$$\mathbf{B}(p+1)=\mathbf{B}(p)-\frac{\operatorname{grad}_{\mathbf{B}(p)} Q}{(\mathbf{H}(\mathrm{Q})+\lambda \mathrm{I})} \tag{11}$$

where I is the unit matrix and λ time-varying factor weighing between the Newton–Rapson method and the steepest descent method [2].

2.3. POWER SYSTEM MODEL

Training data set consists of examples of current waveforms and the corresponding target magnitudes taken from the steady state. Aforementioned waveforms were recorded for faults in 110 kV line modelled in EMTP (Fig. 2) under analog filtering with 330 Hz cutoff frequency and sampling frequency of 1 kHz. Additionally, training current waveforms were artificially distorted with harmonics of maximum magnitudes as given in Table 1.

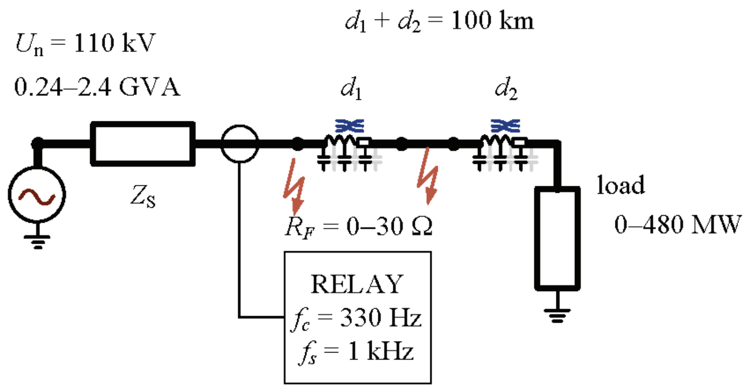

Fig. 2. Modelled 110 kV system

Table 1. Accepted levels of harmonic distortions for nominal power system conditions

$h_{\#}$	I [A]
2	40
3	70
4	25
5	30

3. RESEARCH OUTCOMES

The estimator (1-2) underwent optimization for different lengths of the transient states with parameter M varied from 0 to 20. The maximum relative errors of measurements with respect to maximum error of algorithm (1) based on the full cycle Fourier filter were evaluated for all received optimal estimators. The errors were compared on the basis of the same set of fault cases, yet unused for the optimization.

Figure 3 illustrates the unit impulse response of two filters obtained for the adopted 7 samples length of the transient state. As one can see, the windows of these filters are neither symmetric nor anti-symmetric, so that the phase characteristics of these filters are non-linear. However, the fundamental component magnitude estimation according to (1) does not require linearity of phase displacement in wide range of frequency yet only calls for both filters to have the same value of magnitude and constant relative phase shift equal to π/2 for close proximity of 50 Hz (47 Hz–52 Hz). Furthermore, both characteristics (phase and magnitude) for higher frequencies should be shaped to provide a compromise between the expected response rate estimator (1) and its accuracy (eliminating the impact of harmonics) for samples of steady state i.e. for n exceeding $M + N$. The frequency responses of both optimized filters for $M = 7$ are shown in Fig. 4.

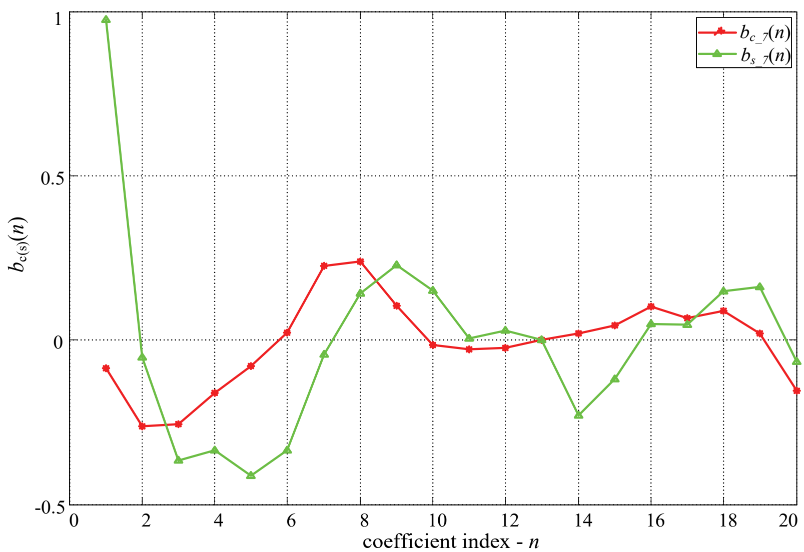

Fig. 3. Unit imulse response of filters optimized for $M = 7$

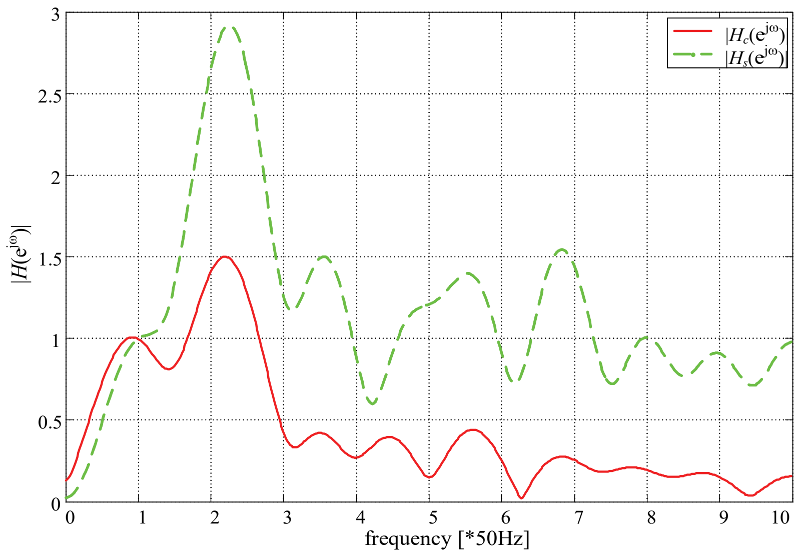

Fig. 4. Frequency response of filters optimized for $M = 7$

Figure 5 presents example estimate of current magnitude for the ground fault in 110 kV line. In addition, estimates realized with the conventional algorithm (1) based on full cycle Fourier filter and based on original and differentiated signal are depicted. As one can see, the response of the optimized estimator shows its immunity to the decaying DC component as well as its rapid reach of the steady state magnitude. The shortening of the estimation transient state duration when compared to response of the conventional algorithm can be assessed to about 12 samples, i.e. 12 ms.

The performance analysis of the three aforementioned measuring algorithms carried out based on the testing signal set allowed for determination of their upper and lower response bounds. Envelopes of response families for unified currents of analyzed estimators are depicted in Fig. 6. It also gives definition of the maximum relative errors used to prepare Fig. 7.

Analyze results for all investigated estimators for M varied from 0 to 20 samples are presented in Fig. 7. The diagram shows that estimators designed for the adopted signal model resulting from fault conditions modelled in 110 kV are characterized by a smaller maximum error starting from $M > 7$ when compared with conventional measuring algorithm. Figure 7 also shows that expanding the length of the transition state above $M = 9$ only slightly reduces the maximum relative errors. The error, as compared with the conventional algorithm, can be for $M = 20$ reduced to about 0.45.

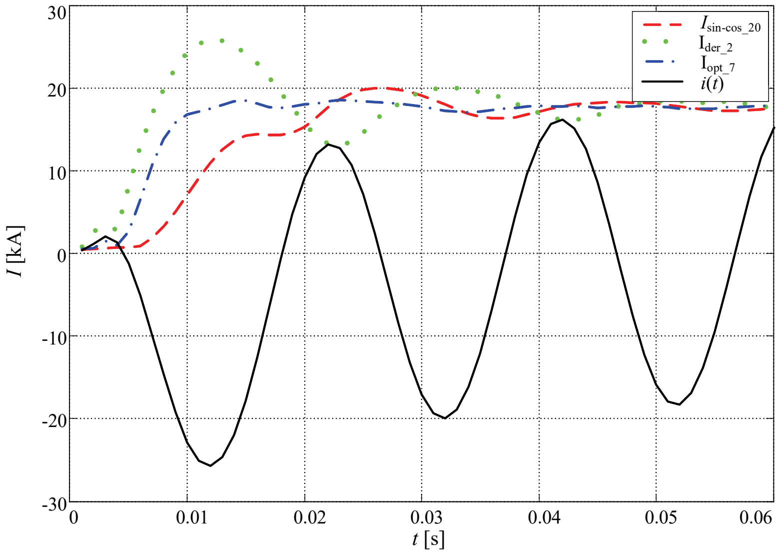

Fig. 5. Current magnitude estimations based on formula (1)
with the use of full cycle Fourier filter,
orthogonalization by signal differentiation, and optimized filters obtained for $M = 7$

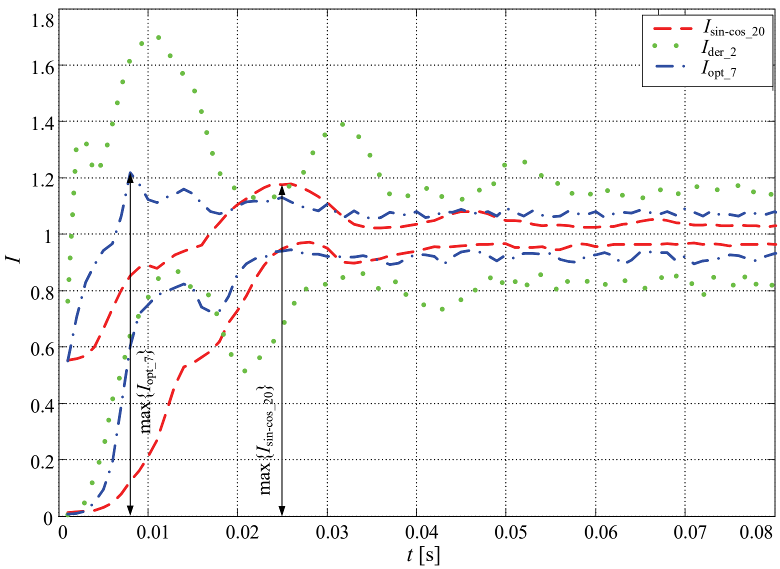

Fig. 6. Transient response limits of the magnitude estimator
based on the full cycle Fourier algorithm,
signal differentiation based algorithm, and the algorithm optimized for $M = 7$

Similar studies were carried out for algorithm optimized for maximum length of the response transient state of 20 samples. The corresponding impulse and frequency responses of the filters are shown in Figs. 8 and 9, respectively. As one can see from comparison of Figs. 5 and 9, resignation from forcing the rapid response allows for better filtering of high frequency components in particular 2nd and 3rd harmonic. The

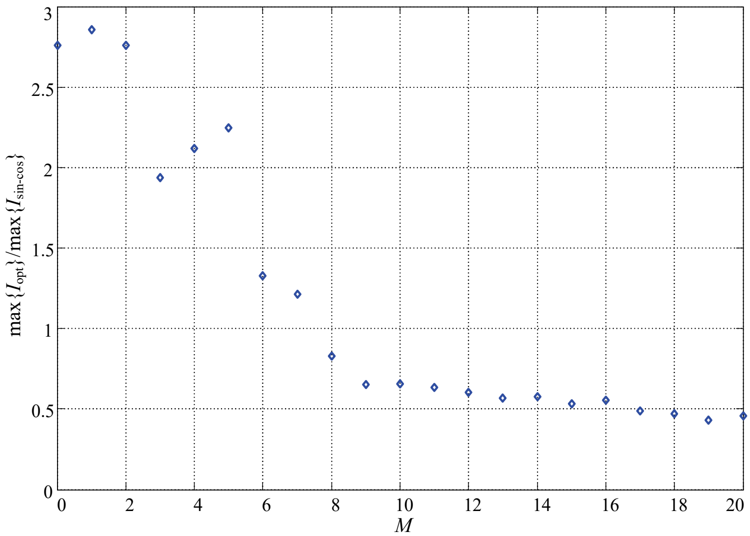

Fig. 7. Maximal relative estimation errors with respect to the error of full cycle Fourier algorithm versus the length of the transient state of M samples

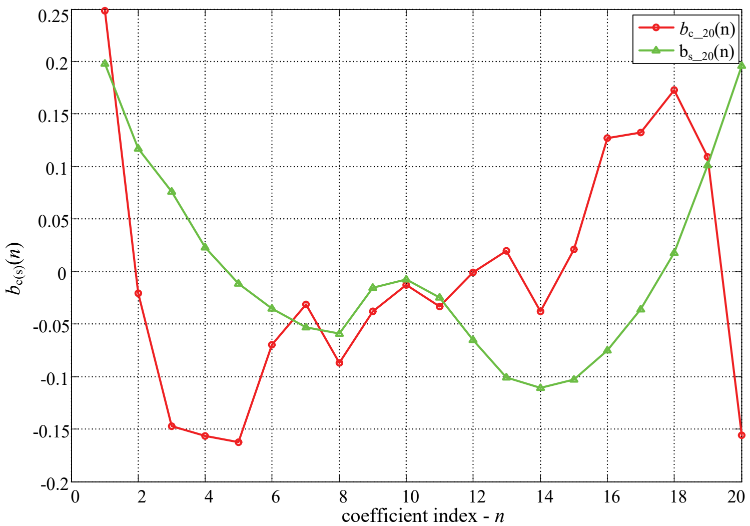

Fig. 8. Unit impulse response of filters optimized for $M = 20$

effect is clearly visible as small errors in the steady state, i.e. narrower envelope in Fig. 10 vs. Fig. 6. However, the ability to eliminate the effect of the decaying DC current component in both temporary and steady state has decisive influence on the quality indicator presented in Fig. 7.

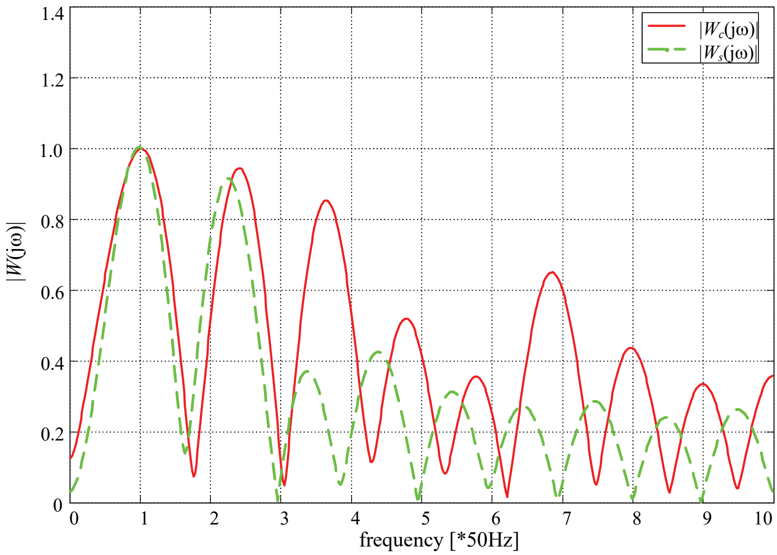

Fig. 9. Frequency response of filters optimized for $M = 20$

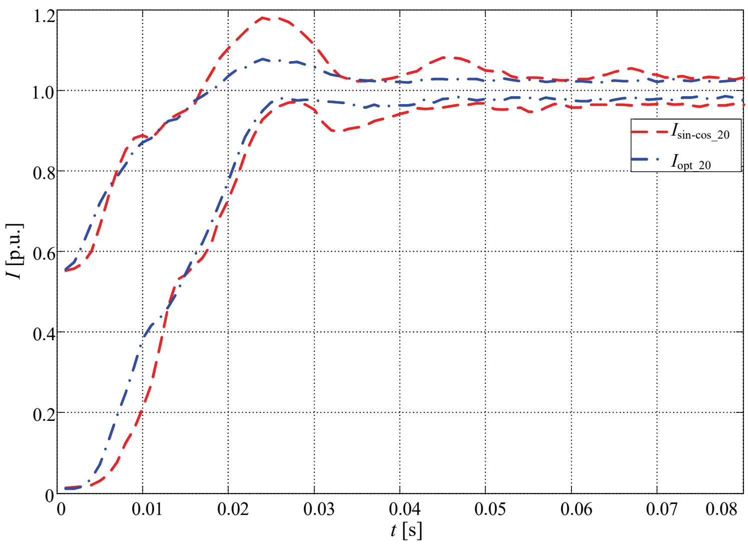

Fig. 10. Transient response limits of the magnitude estimator based on the full cycle Fourier algorithm and the algorithm optimized for $M = 20$

3.2. FREQUENCY DEVIATION IMPACT ON MAGNITUDE ESTIMATION

Since the system frequency undergo continuous fluctuations and is not constant in long time intervals, all estimators of electrical quantities such as magnitude, impedance etc. should be insensitive to frequency deviation in the vicinity of the nominal system frequency. Occurring system frequency variations should not exceed the limits of 49.5 Hz to 50.2 Hz for normal conditions of the power system, however variations in the range 47.0 Hz to 52.0 Hz are accepted.

Figure 11 shows errors of magnitude measurement of purely sinusoidal signal as the function of frequency. As can be seen the error of estimation is zero for full cycle Fourier algorithm, yet only for 50 Hz. The accuracy of this algorithm decreases the deviation pulse, but is still higher when compared with estimates based on the filters designed by means of proposed technique. The accuracy of the conventional method is greater in the frequency range from about 49 Hz to 50.4 Hz. Outside this interval the measuring algorithm based on filters optimized for $M = 7$ is more accurate. One may also notice a relatively higher resistance of the algorithm based on filters optimized for 20 sample transient state. In this case, estimation errors are less than 1% for the frequency deviation of ±3 Hz.

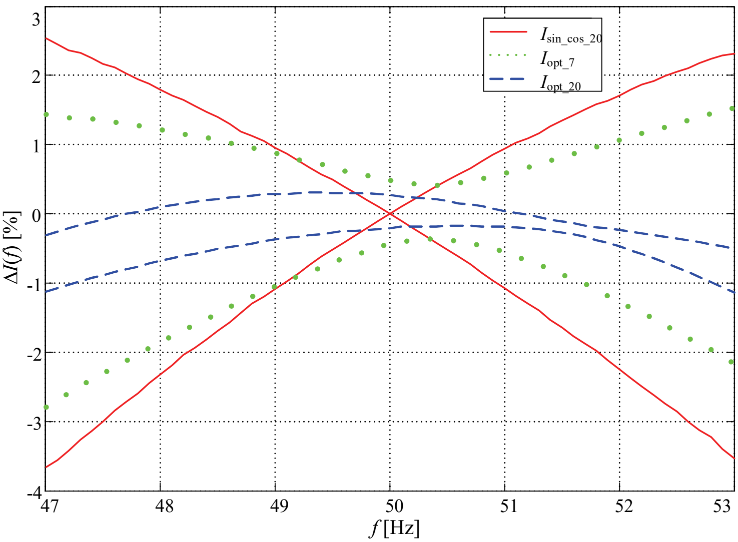

Fig. 11. Magnitude estimation errors vs. deviation of the system frequency

4. CONCLUSION

The paper presents optimization method of magnitude estimators intended for instantaneous overcurrent protections. Assumptions regarding the project were primarily to ensure the prompt estimator response after a fault inception and simultaneous reduction of transient state errors resulting mainly from the decaying DC current component.

By appropriate choice of the signal model, the proposed approach allows for arbitrary forming of magnitude characteristics of the filters. This selection is carried out by selection of the power system model determining transient states of electrical phenomena, the appropriate choice of the fault phenomena model, i.e. arc model, interferences occurring in the normal operation of the power system as well as the impact of instrument transformers on protection quantity wave shapes.

REFERENCES

[1] MITRA S.K., KAISER J.F. (eds.), *Handbook for Digital Signal Processing*. John Wiley & Sons, Inc., New York 1993.

[2] MARQUARDT D.W., *An algorithm for least-squares estimation of nonlinear parameters*, Journal of the Society for Industrial and Applied Mathematics, 1963, 11(2), 431–441.

smart power grid, digital security, risk analysis, hazard valuation, cyber-physical security.

Robert CZECHOWSKI*

CYBERSECURITY RISK ANALYSIS AND THREAT ASSESSMENT WITHIN SMART ELECTRICAL POWER DISTRIBUTION GRIDS

Development of electrical power systems and their integration with an increasing number of smart automation devices compel to undertake a new approach to the issue of the system's security. Reliability of an electrical power system and high service availability are the essential characteristics of efficient strategic electricity customers, i.e.: large industrial facilities, railway transport, medical service providers and life-saving institutions. The time of manual or automatic system recovery after a failure, which increases its security, is not without significance, either. The article discusses the issues of risk assessment and management, including the overall process of analysis and assessment of threat probability in electrical power systems.

1. INTRODUCTION

The beginning of the XXI century marked rapid development of digital technology in critical systems, which gave them brand new significance to efficient and secure functioning of a country. Systems with extensive structure and range of their functionality, such as: fuel distribution, drinking water supply, mass media and communication, and especially electricity suppliers, currently constitute the most important branches of economy, and disruption of their operation might put a country or its citizens at risk of serious consequences. During the last twenty years, protection of these systems has become very important due to increasingly complicated infrastructure and new threats. These systems also pose a challenge for their designers.

Potential system failures (regardless of the system's current technological level) directly determine the system's efficiency, but also indirectly – scope of the impact

*Wrocław University of Science and Technology, Department of Electrical Power Engineering, Wybrzeże Wyspiańskiego 27, 50-370 Wroclaw, Poland, e-mail: robert.czechowski@pwr.edu.pl

which influences bodies using the system's services. Making strategic decisions on designing, managing and developing an electrical power system can significantly influence a country's functioning and development perspectives in the future, and especially be of importance for its security and international position, as well as its economic and defensive potential. Moreover, political turmoil, conflicts and international crises occurring in certain regions can directly impact a country's energy security. Another possible cause of a crisis constitutes actions rooted in sabotage, and threats originating from third parties, like acts of terrorism.

Supply of electrical energy by use of a smart grid is increasingly often tied to digital information flow, allowing for both continuous monitoring of the demand, and control of the grid itself. In effect, it will directly translate into its increased efficiency. Such solutions allow for flexibly shaping the demand and adjusting the supply to daily requirement. Combined with utilization of energy-efficient devices, smart solutions and fully automated technological processes, it will increase energetic efficiency of the entire system. To a certain degree, these solutions will also limit potential risks related to failures or intentional attacks. Recently, more methods and technical measures have appeared to aid in system operation optimization and minimizing potential effects of disrupted system operation. They include such actions as: risk analysis and threat assessment, created for the needs of centralized management. In order to effectively utilize the aforementioned methods, it is essential to sweep the supervised system and identify threats whose removal requires nonstandard procedures and resources. It is worth mentioning that risk (lat.: *Risico*) is a possibility to make profit or sustain losses as a result of a certain action, and threat assessment means evaluation of a given threat's impact based on its origin, duration, effects and determination of resources necessary to neutralize it. Among the many definitions, the most adequate one, in the context of an electrical power system, is operational risk which constitutes possible adverse effects of computer system errors or organizational errors.

Risk estimation and threat assessment methods allow to notice and take preventative action, as well as determine the degree of security improvement in an electrical power system as a result of the undesirable situation. On one hand, the decision maker has to consider purely technical solutions, on the other – consequences resulting from possible discredit of the system and lost trust for a given operator.

2. STRATEGY

The general security strategy for smart grids assumes both common and specific needs for individual infrastructure parts, i.e.: security of information, data bases and technological process visualization. The main tasks of cybersecurity strategies are making employees aware of potential threats and taking action in order to prevent them. Nevertheless, a strategy to react, mitigate the effects of a failure or cyberattacks, and make a full system recovery should be developed in case of a cyberattack against an electrical power system.

Implementation of a security strategy requires determination and implementation of a specific threat assessment process dedicated to assure cybersecurity of an entire smart electrical grid. The associated risk concerns probability of an undesirable incident or event, as well as related consequences. Organizational risk can encompass many kinds of risk (e.g.: risk related to investment, budget, strategy management, legal responsibility, automation digital security, inventory and information systems). The most common causes of increase and emergence of risk are:

- human errors – losses sustained due to human mistakes inside the company or mistakes of external employees (e.g. customer extortion),
- process errors – losses reflecting potential weaknesses in procedures,
- poor work organization – risk resulting from e.g. changes implemented into management or communication methods,
- technological errors – equipment failures, software errors, network outages or failures of other kinds of technology, as well as loopholes in security measures of IT systems,
- external causes – legal proceedings or natural disasters.

Risk assessment process in a smart grid is based on existing ways and methods of risk assessment devised by the private and public sectors, and it encompasses identification of consequences, vulnerability to attacks and threats. In order to assess risk in relation to a smart grid, their protection has to be flexible and include coexistence of all components of the system, as smart grids encompass systems from sectors of IT, telecommunication and energy. Risk assessment process concerns all three sectors and their interaction with smart grids and smart metering. All in all, priority goals of IT system security measures include confidentiality, as well as integrity and accessibility. In industrial control systems, including power systems, accessibility takes priority over all security measures, then comes integrity, and then confidentiality. The goal of risk management process is also indication of so-called strategic goals – determining what actions should be taken in order minimize the possibility of a threat or its consequences. Fig. 1 shows exemplary components and course of action, which can be as follows:

- threat analysis – indication of where threats can be found, description of their scenarios,
- prevention – determination of a strategic goal, undertaking ventures necessary to achieve the strategic goal, and the necessary forces and resources,
- preparation – determining where locally, regionally and nationally implemented programs are indicated, whose goal is increased security,
- response – determination of response principles, as well as response priorities in case of threats,

– historical data analysis – analysis of crisis events that have taken place in the past (according to the following parameters: date or time interval; place/area of appearance; short description; consequences of the loss),
– conclusion analysis – analysis of conclusions derived during the preceding events related to the analyzed case.

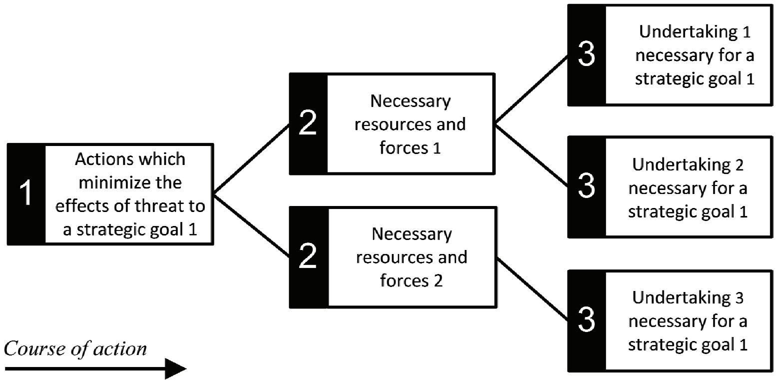

Fig. 1. Chart of threat analysis and estimation process' organization.
Legend: 1 – analysis and plan of action, 2 – determination of forces and resources for a strategic goal, 3 – realization of the strategic goal.

Awareness of borne risk is definitely very important in decision-making on the financial market. Sometimes, however, it is worth taking risks, as it often turns out that greater risk leads to potentially greater profit (sadly, also greater possible loss). The possibility to make above-average profit is enough of a temptation for some financial institutions to decide to take the risk, exposing themselves to possible losses. In line with the act on crisis management [1], these goals have been ordered according to their importance and the ones that take priority from the perspective of national security have been indicated. For all strategic goals, the indicated elements are strength and resources necessary to achieve them, as well as ordered undertakings which must be realized in order for a strategic goal to be achieved.

3. RISK ANALYSIS AND ASSESSMENT

In analysis of consequences for critical infrastructure, it is determined – if and how a given scenario influences the functionality of a given critical infrastructure and if there is a potential threat to the system. In line with the act on crisis management [1], critical infrastructure is understood as a system and interrelated functional objects that constitute it, including construction objects, telecommunication equipment, telecommunication installations and other services crucial for the security of a country and its citizens. The constituents also aim at ensuring proper functionality of public administration bodies, as well as institutions and businesses. Still, each critical infrastructure is very important from the perspective of security of a country's operation, especially: mass media service providers, water and energy fuel suppliers – the most important of them are electrical power systems. Such a strong and high position of electrical power systems is caused by virtually every branch of economy being reliant on the supply of electricity. From this point of view, the infrastructure of creation and distribution of electricity encompasses nearly all systems, from communications systems, teleinformation networks, financial markets, healthcare and rescue, to logistics systems (Fig. 2).

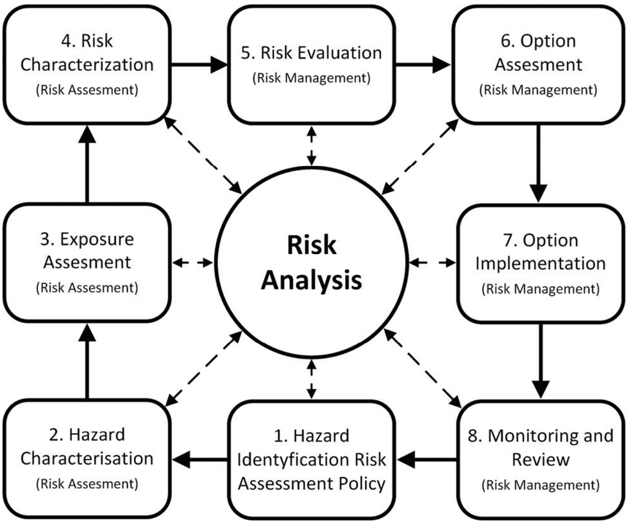

Fig. 2. Diagram of risk analysis process.
Diagram of communication between participants and agents

Risk analysis process is also a pre-determined course of action which is described in directives or internal documents of a given company. The analysis procedure can be written, graphical or tabular, based on which a given scenario has been developed. It is also recommended to include a map indicating the area and reach of a potential threat, separate for each scenario [2]. From the formal perspective, the document should include all important information that may influence the final assessment and outcome of risk estimation. Detailed risk analysis should be divided into individual analytical, decision-making and implementation stages. The most important constituents of risk analysis and estimation, although not the only ones, are entry parameters (stage 1) which include:

- threat monitoring, warning and alarm system,
- threat characteristics and assessment of its occurrence risk,

– risk map and threat map,
– list of tasks and responsibilities of crisis management participants in the form of security grid,
– list of strengths and resources available for use in crisis situations,
– crisis response procedures determining the course of action in crisis situations,
– plan of communication and power organization in case of cascade failure,
– principles and procedure of damage assessment and documentation,
– procedures of initiating energy reserves,
– principles of informing the population of threats and course of action in case of threats [3].

After the probability and consequences have been determined, it is possible to indicate the risk value (stage 2). Risk value for each scenario is indicated on the risk matrix showing the dependence between probability and consequences (Fig. 3). Visualization is not only helpful in quick classification of a given event, it also allows for reading the distribution of most critical situations in relation to their probability.

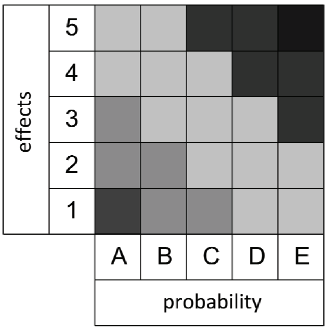

Fig. 3. Risk values have been color-marked:
from minimal (A1) do extreme (E5)

Another stage is a process of risk acceptance (stage 3) within category 4:

– accepted risk (A) – no additional security measures are required, current solutions and their assigned forces and resources are accepted, standard monitoring actions are undertaken,
– tolerated risk (acceptable) (B) – assessment should be made of other solutions or possibilities to implement small organizational, legal or functional changes which will contribute to security improvement,
– conditionally tolerated risk (C, D) – additional security measures should be implemented within a certain period and the utilized solutions should be improved,
– unacceptable risk (E) – immediate action should be taken to assure and improve security, and to implement additional or new solutions.

In the final stage, justification of risk acceptance level should be made (stage 4). Occurrence frequency is often based on historical data and shared experience with bodies undertaking similar activities. Government crisis response documents are often the source of risk estimation concept [3]. Potential threats can be classified as follows:

– very rare (1) – the event might occur only in exceptional circumstances,
– rare (2) – it is not expected for the event to happen, prior occurrence of the threats has not been documented in similar organizations or reports made after an incident. There is little chance, reason or other circumstances for the event to happen,
– possible (3) – might happen in a certain time and conditions, rarely by accident, events are sometimes documented entirely or most often partly. There is some chance, reason for the event to happen,
– probable (4) – there is a probability that the event will take place in specific circumstances, such events are systematically documented, and information on them is provided. There is a specific reason or cause for which the event takes place,
– very probable (5) – the event is expected to happen, it will take place in most circumstances, and such events are well documented [4].

Risk analysis and estimation is a very complicated process which requires not only synthetic knowledge of its creation methodology, but also practical industry knowledge both appropriate and required by a given system. The greatest problem for designing an analytical model aimed at helping with decision-making is estimation of potential threats' impact and preparation of adequate solutions, taking priorities, means and system recovery time into account.

4. CYBERATTACKS AND ELECTRICAL POWER GRID FAILURES

Presently, cybernetic threats we deal with in today's world are characterized by high precision and sophistication. In terms of extensive electrical power systems, it means that critical systems must be systematically monitored and analyzed in case of threats, also in the form of an intentional attack. Large-area electrical power grid failures caused by destructive actions of third parties is the worst possible scenario. Such an attack may target the entire energy sector – power plants, thermal power plants, transmission and distribution networks, even low-voltage networks. High vulnerability of a system to damage and attacks might cause very spectacular and costly failures which include:

– large-area electrical power grid failures – network failures cause by weather factors in large concentrations (natural disasters), causing serious disruptions in electricity supply throughout larger areas.

– widespread long-term system blackouts – dysfunction of the electrical power system of a country or its significant portion – disappearance of energy supply ability to a large number of consumers in sufficiently long time or weather conditions.
– power deficit – limitations in electricity supply and consumption caused by a shortage of production capacity in state system power plants or resulting from limited transfer capabilities [4].

The contemporary grids' problems detailed above are events most often caused by spontaneous damage of elements in an electrical power grid and system, related to impact of weather factors – causing local disruptions in electricity supply. In recent years, however, a brand new threat, related to actions of third parties, has emerged – cybernetic attacks – they are some of the most effective and most bothersome (as far as damage goes) actions striking against an electrical power system's operation security and its related cooperative bodies, and electricity consumers. Cyberterrorism is becoming an increasingly common method, as the only things necessary to undertake cyberattack-related actions are a computer and World Wide Web connection. It is worth mentioning that the cyberspace has no control barriers, but the attacker's experience plays a significant role, as they not only need ICT and programming knowledge, but also industry knowledge specific for the attacked system. Attack targets may vary vastly – from an operator's system management center, to transmission and distribution networks, to low voltage networks – electricity meter grids and smart home gateways controlling local automation and receptions. The probability of discovering loopholes in a seemingly secured electrical power system is relatively high. This is evidenced by media reports on subsequent large-area failures (or attacks), such as: Pakistan (26 January 2015) [5], Kuwait (11 February 2015) [6], the Netherlands (27 March 2015) [7], Turkey (March 31, 2015) [8], USA, Washington, Spokane County (November 17, 2015 [9]), Crimea (21 November 2015) [10].

Poland is not currently among countries targeted by terrorist attacks. However, because of the country's international activities, like participation in Afghanistan operations, policy of cooperation with the USA, the risk of a terrorist attacks against strategic objects, including critical systems, cannot be completely ignored. The common causes of failures include the human factor (ignorance, disregard for regulations, bribery, frustration, ideology), system and data modification, organizational and technical errors, sabotage, damage or theft of transmission elements, which might lead, among others, to:
– disruptions in functionality of hydro-technical infrastructure devices,
– disruptions in communication infrastructure: urban, rail and air,
– disruptions in functionality of communications systems and teleinformation systems: limitation or complete loss of radio and phone communications, threats to proper functionality of an IT system,
– hindered information flow and no access to data necessary for security and public order services to work,

– suspension of border checks of passengers, transports,
– failure of a banking system and non-cash transactions,
– no functionality of central accounting systems,
– lack of or limited telecommunications or mail services.

Cybernetic security of electrical power systems covers all issues related to automation and communication, which influence functionality of the tools governing these systems. It also includes tasks of prevention, mitigation of consequences, as well as facing other cybernetic terrorist events.

5. CONCLUSIONS

The considerable degree of complexity of electrical power systems, which has become especially apparent in the recent years, inclines to take a brand new look on security of electrical power systems. Except for procedures described in a security policy, decision-making should be also supported by decision models of risk analysis and estimation. These models are a valuable tool for making decisions in situations with uncertain or difficult to predict results. Risk estimation process allows the decision-maker to make a final decision based on historical data, current status, expected profit or possibility of potential losses. Based on analysis of many cases, a system designer or a person responsible for the security of an existing system can determine and estimate risk accompanying normal operation of an electrical power system. It requires the decision-maker to constantly monitor the system and be ready to devise emergency plans and quick response in case of threats to the project's success. If there are no formal courses of action prepared for potential decisions, an attempt should be made to prepare a formal document based on historical data, containing a description of action for e.g. when risk is acceptable and when it should be reduced. Decisions should be made along with the entire team responsible for risk management in the company, especially with people responsible for management of the entire organization, not just the security segment. Risk estimation models dedicated for electrical power systems are the second (after the security policy) most important element constituting security of the system's operation. Risk estimation involves convincing our consciousness to make more accurate decisions regarding the state of system security, and then undertaking certain preventative actions, all the while having the organization's main goal in mind, which is most commonly maximizing profit and minimizing losses. As a result of risk analysis, we can conclude what threatens the security of our system and what the consequences of these hazards coming to life may be. The described methods also allow to decide what to do with identified and classified risk. It should be remembered, however, that effective risk management requires adequate analytical knowledge, time and often significant financial resources.

This paper was realized within NCBR project: ERA-NET, No1/SMARTGRIDS/2014, acronym SALVAGE. “Cyber-Physical Security for the Low-Voltage Grids”.

REFERENCES

[1] Dz.U. 2007 nr 89 poz. 590, *Ustawa z dnia 26 kwietnia 2007 r. o zarządzaniu kryzysowym*, Tekst ujednolicony: D20070590Lj.pdf, 2007.

[2] UNDERBRINK A., *Risk Analysis in Distribution and Transmission Networks*, ABB AG, Mannheim, Germany, 9th International Conference on Probabilistic Methods Applied to Power Systems KTH, Stockholm, Sweden, 2006.

[3] Rządowe Centrum Bezpieczeństwa, *Ocena ryzyka na potrzeby zarządzania kryzysowego. Raport o zagrożeniach bezpieczeństwa narodowego*, Warszawa 2013.

[4] Rządowe Centrum Bezpieczeństwa, *Procedura opracowania raportu cząstkowego do Raportu o zagrożeniach bezpieczeństwa narodowego*, Warszawa, 2010,

[5] Sky News, *Militant Attack Plunges Pakistan Into Darkness*, http://news.sky.com/story/1414477/militant-attack-plunges-pakistaninto-darkness (access date: 22.03.2016), 2015.

[6] Mail Online Wires, *Most of Kuwait hit by Power Blackout*, http://www.dailymail.co.uk/wires/afp/article-2949576/Most-Kuwaithit-power-blackout.html, (access date: 22.03.2016), 2015.

[7] ESCRITT T., Reuters, *UPDATE 5-Power returns to Amsterdam after outage hits a million homes*, http://uk.reuters.com/article/dutch-poweroutages-idUKL6N0WT1DI20150327, (access date: 22.03.2016), 2015.

[8] RT Question More, *Turkey struck by biggest power cut in 15 years, investigation underway*, https://www.rt.com/news/245529-massivepower-outage-turkey/, (access date: 22.03.2016), 2015.

[9] FOX News Weather Center, *Tens of thousands shivering without power in Washington City*, http://www.foxnews.com/weather/2015/11/24/tens-thousands-shiveringwithout-power-in-washington-city/, (access date: 22.03.2016), 2015.

[10] RT Question more, State of emergency, *Blackout in Russias Crimea after transmission towers in Ukraine blown up*, https://www.rt.com/news/323012-crimea-blackout-lines-blown-up/, (access date: 22.03.2016), 2015.

static and dynamic model, price,
isolated system, Fisher equation, transient processes.

Valeri ZHUIKOV*, Julia YAMNENKO*,
Tetyana TERESCHENKO*, Liubov KLEPACH*,
Ivan BOIKO*

STATIC AND DYNAMIC TARIFFING ELECTRIC POWER AUTONOMOUS MICROGRID

The paper presents a static model of the price calculation for the various alternative electricity sources, and includes technical and economic performance of different energy sources for the guaranteed power. The table with calculated technical and economic indicators for various alternative energy sources is provided. The presented dynamic model which unites energy indicators of power generating systems and economic indicators of the closed macroeconomic system because price regulation on the power market of Ukraine happens in a statics. That's why not allowed to perform an assessment of dynamic change of the tariff price of the electric power in the local isolated systems. When abrupt change isolated power generating capacity of the system is changing the tariff price of electricity cannot be taken into account when using static models. An example of the isolated system consisting of the diesel generator and the consumer is reviewed. The model allows to research influence of transition processes of the generator on change of cost indicators of an economic system, and also to estimate the adequate tariff price both for the producer, and for consumers of the electric power. This model is modelled in Matlab.

1. INTRODUCTION

At development of the system of management of power supply of knots of the distributed generation the combination of the centralized and decentralized management can lead to contradictions with tasks which minimize consumption of other resources (water, gas, etc.) [5], [15]. Therefore it is necessary to choose criterion of efficiency which would be the general for various problems of management and I allowed to carry out a complex assessment of a condition of system of power supply of local ob-

* National Technical University of Ukraine "Kiev Polytechnic Institute", Faculty of Electronics, Department of Industrial Electronics, 16, Polytechnichna str., off.313, Kyiv, 03056, Ukraine, e-mail: luibaklepach@gmail.com

ject of Micro Grid. Such criterion is the integrated cost parameter which allows estimating the direct and mediated expenses necessary for development and consumption of electric energy, and losses from her inefficient use.

Because as criterion cost is used, it is expedient to apply the theories developed in economic branches [2], [6], [10] to realization of optimum behaviour of system. Then the problem of optimization is reduced to the joint solution of the equations describing electromagnetic processes in technical devices and the equations considering cost factors [4], [7]. As target functionality which value has to be minimized the cost of energy which pays off as amount of energy, increased by the corresponding tariff operating in this interval of time is chosen. The accounting of tariffs it is necessary as only existence multitariff systems of payment gives the chance to lower expenses by transfer of intervals of work of separate loadings of intervals of lower tariffs, and the moments of turning on of alternative generators – in intervals of higher tariffs of a network. The modern technological level allows to apply the current tariffs for the electric power of a network [1] to realization of formation of more flexible management with feedback and an assessment of a condition of the operated objects.

Optimum function of management which allows providing performance of the set useful work as loadings with minimization of expenses is result of the solution of a task. Optimum function of management represents set of values of the operating parameters in the set time intervals.

For the purpose of the accounting of cost factors (processes of consumption, production, the budgetary restrictions) by development of systems of management of power supply of knots of the distributed generation the electro technical equations are combined with the equations borrowed from the economic theory [2]–[4], [6], [7], [11]–[13]. Such combination leads to creation of electro-cost models which, except definition of currents and tension of electro technical objects of Micro Grid, the minimization of cost costs of service and use of these objects allowing solving a problem.

The model of the general equilibrium allows describing and solving a wide range of the problems arising at management of power consumption in a common market of MicroGrid.

With the development of the Smart Grid technology [16] there are widespread isolated systems, including power generation systems based on diesel generator. Regulation of electricity prices now is not dynamic, and based on the set value [16], [22]. There are many available methods for a spot forecasting, for example, presented in [23], which produces forecasts for the electricity price in the spot market, for a term of 24 hours and can be used for the spot trade optimization. Another method for a electricity price forecasting is pointed in [24], where a single-hour and 24-hour models are used to study the electricity price forecast. For a fixed hourly tariff price, availability a considerable part of transients in the base period of time causes significant deviation of actual established tariff prices, that leads either to a lack, or an excess of money in the system. The apparent actuality creating a flexible dynamic tariffication that will provide a money balance between consumer and producer of electricity.

The problem of the development of dynamic tarrification rose much earlier, for example in [25] presented an integration of consumer and utility, applications oriented theoretical models, for the purpose of establishing an overall systems approach to the behavior and interaction of the participants in a dynamic tariff environment. This method assumes that industrial loads which can be started or stopped without technical limitations, so the starting and stoping times are so short that they can be taken as zero. Another method presented in [26] is based on dynamic models to correctly incorporate the fundamentally dynamic nature of power system regulation and incentive the corresponding desirable actions. In [27] presented a dynamic pricing strategy for Smart Grid. The objective of this strategy is to discourage concentrated electricity usage and flatten peak load in the power system. The price is subject to multiple factors such as location, time, and usage. Current pricing strategy links the price to time and location only and ignores its usage-dependent nature. The methods considered above do not take into account the influence of transient processes when switching operating modes. It is obvious that the duration of transient processes in generator has a direct impact on the cost parameters of an isolated system, i.e. the deviation of actual tariff price of electricity from that accepted by static values set out in the existing model of hourly billing. As a part of the introduction of a flexible tariffication we need a dynamic electro-cost model that combines energy and economic indices of the closed power generating system, consisting of a generator and consumer, that allows to explore the impact of transients generator to changing value indicators of the economic system and calculate an adequate tariff price for producers and consumers.

The rest of this paper is organized as follows. Section II describes the general principles of creation of electro-cost models. Section III is devoted to the static model of the isolated electro-cost system. Section IV illustrates the dynamic model isolated electro-cost system. Section V shows the research of transition processes in system. Section VI is dedicated to conclusions of the paper.

2. GENERAL PRINCIPLES OF CREATION OF ELECTRO-COST MODELS

At creation of control algorithms of power supply of knot of the distributed generation taking into account cost factors the greatest interest is caused by the theory of the general equilibrium [6] which allows formulating conditions of the most effective management of power supply with providing the minimum cost expenses in a common market of production and consumption. From positions of the economic theory products produced and consumed in the market of the local system (Fig. 1) is electrical energy. The electric network and alternative generators, being a part of system, carry out a role of producers of production, and loading-her consumers.

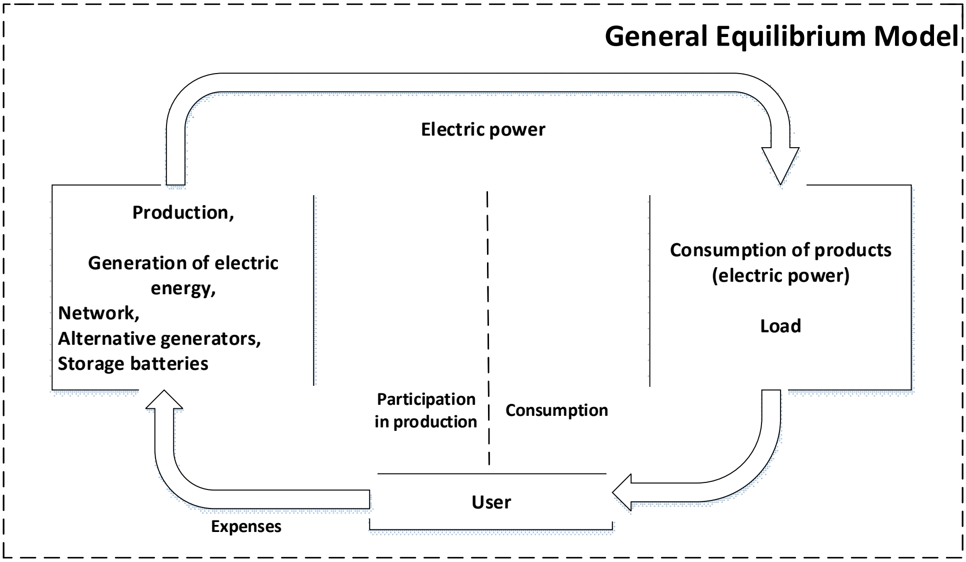

Fig. 1. The balance of production and consumption

For each electro technical device (the generator or the consumer of energy) it is necessary to solve the optimum problem in the field of minimization of expenses with ensuring efficiency of functioning. Set of separate optimizing tasks allows to formulate a problem of the general equilibrium and to define the most expedient strategy of adaptation of management both separate devices, and all system taking into account the expenses necessary for maintenance of this balance in the system providing optimum use of energy [6].

Electro-cost model of the general equilibrium in a common market of production and consumption of electric energy:

$$\begin{cases} \dfrac{dX(t,\Delta W,\Delta \$)}{dt} = A(t,\Delta W,\Delta \$)X(t,\Delta W,\Delta \$) + U(t,\Delta W,\Delta \$) \\ \Delta W = \sum_{f=1}^{F} W_j^f - \sum_{h=1}^{H} W_j^h \to 0, \quad j = \overline{1,n} \\ \Delta \$ = \sum_{f=1}^{F} r_i^f - \sum_{h=1}^{H} r_i^h \to 0, \quad i = \overline{1,m} \end{cases} \tag{1}$$

where H and F – number of consumers and sources in compliance; W_j^f and W_i^h – the amount of energy, makes each generator f and each consumer of h respectively consumes, ΔW – excess of the developed energy which can't be used that defines a condition $\Delta W \to 0$; r_j^f and r_i^h – volumes of expenses of i a look, $i = \overline{1, m},$ necessary for electricity generation by each generator f and for functioning of the consumer of h.

Under a common market of production and consumption in this context set of the devices making and consuming energy and also channels of an exchange of energy at the certain tariff rates (prices) means.

Use of the given models allows describing the technical and economic processes proceeding in separate components of electro technical object of Micro Grid, interaction between them, and also the general behaviour of object is realized for achievement of an overall objective of ensuring effective management of power supply.

3. STATIC MODEL ISOLATED ELECTRO-COST SYSTEM

For quantitative estimation and comparison of different energy sources in uninterruptible power supply system the generalized method is used for estimation of most important parameters common for considered sources [2], [7], [11].

1) **Specific equipment cost** of energy supply system:

$$B_{spec} = \frac{K_{eq}}{P_{nom}} \tag{2}$$

where K_{eq} is the cost of equipment set; P_{nom} – nominal power of the system;

2) **Lifecycle** of energy supply system that is regulated by equipment manufacturer for each concrete system separately. On the average, lifecycle of PV cells and wind generators is about 15–30 years. The lifecycle of diesel generators is limited by amount of working hours and depends on the type of equipment, working conditions and other factors;

3) **Consolidated year expenses** for the generation of 1 kW of total capacity per year:

$$Z = \frac{P_r \cdot K_c + C}{P} \tag{3}$$

where P_r is regulatory value of profitability; K_c is common investment; C – expenses for technical support service, maintenance, repair; P – total capacity of supplied object;

The general capital investments of K_c are in turn calculated as:

$$K_c = K_{eq} + K_{pr} + K_m \tag{4}$$

where K_{eq} is equipment set cost; K_{pr} is the value of designing, definition of placement location, and installation; K_m is cost of construction and installation works, installation cost.

The standard coefficient of profitability in (3) is calculated as:

$$P_r = \frac{1}{T_{ex}} \tag{5}$$

4) **Prime cost** of 1 kW*h generated by alternative sources:

$$C_{prime} = \frac{K(t) + C(t)}{W_{gen}(t)} \tag{6}$$

where $W_{gen}(t)$ is total generating power of the system for some period t; $K(t)$ – expenses for the generation for the period t.

Expenses on generation of energy during t time:

$$K(t) = \frac{K_c}{T_{ex}} \cdot t \tag{7}$$

Total generating power is calculated as follows:

$$W_{gen}(t) = \int_0^t P_{gen}(t)dt \tag{8}$$

where $P_{gen}(t)$ is the power generated for the period t.

So, based on the equations given above, provided $t < T_{ex}$ cost of 1 kWh of electricity generated by power plants on the basis of alternative energy sources is calculated using the following formula:

$$C_{prime}(t) = \frac{\frac{K_c}{T_{ex}} \cdot t + C(t)}{\int_0^t P_{gen}(t)dt} \tag{9}$$

5) **Payback period** of energy supply system under the condition $P_{gen} < P_r$ can be calculated as:

$$T_{pb}(t) \frac{K_c + C(t)}{C_{network} \cdot W_{gen}(t)} \tag{10}$$

where $C_{network}$ is actual tariff for electrical energy from the power network 220 V.

6) **Profit** from system functioning – the difference between the revenue and corresponding expenses:

$$T_{pr}(t) = C_{network\_total} \cdot W_{gen}(t) - K(t) \tag{11}$$

where $C_{network\_total}$ is the tariff for electrical energy from the state power network of public use [8], [10].

For each of types of alternative power sources there would be some distinctions in efficiency assessment. In particular, such distinctions could be caused by the way of energy tracking, or other factors and indicators connected with structural features of different kinds of generating systems.

The prime cost of different AES is calculated by formulas above, and the decision about expediency of their use, sale or purchase of the electrical energy by the calculated prices is accepted.

The analysis of different pricing methods showed the effectiveness of the method of maximizing the current profit based on the demand for the calculation of electrical energy price [11], [12].

Behind this method the price pays off on the following formula [9]:

$$C_{el} = C_{prime}(t) + \frac{N_{pr} \cdot K_{inv}}{100 \cdot N} \tag{12}$$

where N_{pr} is desirable rate of return as a percentage; K_{inv} – it's the size of the invested capital; N – the planned sales volume.

4. DYNAMIC MODEL ISOLATED ELECTRO-COST SYSTEM

With development of the Micro Grid [16] technology the isolated systems which in particular are power generating systems on the basis of the diesel generator [17] were widely adopted. Usually such systems have limited power and limited loadings. Price control to the electric power happens not dynamically so far and proceeding from the established cost. At the tariff price fixed hourly, existence of a large number of transition processes in basic a period causes a considerable deviation of the actual tariff price established that leads either to a shortcoming, or to surplus of means in system. Relevance of creation of flexible dynamic tariffing is obvious that it will allow providing balance of means between the consumer and the producer of the electric power.

Within introduction of flexible tariffing creation dynamic electro – the cost model uniting power and economic indicators of node of the distributed generation, consisting of the generator and the consumer by means of which it is possible to investigate influence of transition processes of the generator on change of cost indexes of object of MicroGrid, and calculations the adequate tariff price for producers and consumers of the electric power is required.

System "the producer–the consumer of the electric power" it is schematically presented in Fig. 2 as the closed macroeconomic system [18] which combines dynamic and economic parts of the isolated system.

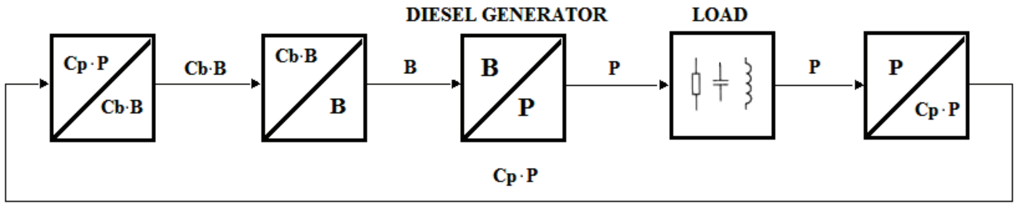

Fig. 2. System "the producer–the consumer of the electric power"

The generator provides electricity power P to consumer, and the consumer pays its cost in the amount of $C_P \cdot P$, where C_P is unit price of power. Generation system spends a certain amount of funds received for the purchase of fuel $C_B \cdot B$, where C_B is unit price of fuel, and a certain amount on their own needs. Received remaining of funds is the profit of the system. The balance of closed power generated system described by the Fisher equation [19] will look like:

$$M \cdot V = C_B \cdot B + C_P \cdot P$$

where M is money supply, which rotates once per time T_V, [uah]; $V = T/T_v$ is number of turns of the money supply M during the analysed period of time T.

Depending on his needs, consumer can increase or decrease the amount of electricity, characterized by level of power, so for some tariff interval Δt change of generated power will be happened, with the balance equation takes the form:

$$M \cdot V = C_B \cdot B + (C_P + \Delta C_P) \cdot (P + \Delta P)$$

Having presented changes in tariff price as: $\Delta C_P = \frac{M \cdot V - C_B \cdot B}{P \cdot \Delta t} - \frac{C_P \cdot \left(1 + \frac{\Delta P}{P}\right)}{\Delta t}$ and considering that $\Delta C_P = \frac{dC_P}{dt} \cdot \Delta t$ an equation received:

$$\frac{dC_P}{dt} = \frac{M \cdot V - C_B \cdot B}{P \cdot \Delta t} - \frac{C_P \cdot \left(1 + \frac{\Delta}{P}\right)}{\Delta t} \tag{13}$$

that describes the dynamic change of the C_P depending on capacity, that provides a per-second tariffication when $\Delta t = 1$ s. Component ΔP will not be used in this study, but it is necessary for the modelling in future tests.

Equation of the capacity expansion for diesel generator is presented in the following form:

$$\frac{dP}{dt} = -\frac{P}{\tau} + \frac{\eta_B}{\tau} \cdot \gamma \cdot B \tag{14}$$

where η_B is efficiency of the generator, γ is conversion factor of fuel produced in power, τ is the time constant for the generator.

The construction of equations (13) and (14) gives a result of a dynamic system which is:

$$\begin{cases} \dfrac{dC_P}{dt} = \dfrac{M \cdot V - C_B \cdot B}{P} - C_P \cdot \left(1 + \dfrac{\Delta P}{P}\right), \\ \dfrac{dP}{dt} = -\dfrac{P}{\tau} + \dfrac{\eta_B}{\tau} \cdot \gamma \cdot B, \end{cases} \tag{15}$$

where $C_B \cdot B = \beta \cdot C_P \cdot P$, $\dfrac{1}{\beta}$ – rate of profit of the economic system.

To reflect the changes in the output of the power generated in the resulting electro-cost model used value ΔB, despite the fact that M and V are close to constant. This assumption is based on the following facts. Money supply M is removed and returned to the system about once per quarter, respectively, studied in a small time interval, number of turns V will change insignificantly. The system (15) will look like:

$$\begin{cases} \dfrac{dC_P}{dt} = \dfrac{M \cdot V}{P} - C_P \cdot \left(1 + \beta + \dfrac{\Delta P}{P}\right) - \dfrac{\Delta B \cdot C_B}{B}, \\ \dfrac{dP}{dt} = -\dfrac{P}{\tau} + \dfrac{\eta_B \cdot \gamma \cdot (\beta \cdot C_P \cdot P)}{\tau \cdot C_B} + \dfrac{\eta_B \cdot \gamma \cdot \Delta B}{\tau}. \end{cases} \tag{16}$$

Thus, received the system that combines electrical and economic parameters of isolated power generating systems with diesel generator, allows calculating dynamic change of the tariff price when changing level of generated power, or vice versa [20], [21].

5. RESEARCH OF TRANSITION PROCESSES IN SYSTEM

Dynamic simulation of transient processes in the system when there is a change and relative to the known initial values, with the parameters listed in Table 1, shows the macroeconomic balance of the system, because, while production power of generator is reducing, unit price of power will grow accordingly. In the absence of restrictions of increases and, after the transient process, corresponding values will be at levels optimal for the condition of the balance in Fisher equation. Simulation results are shown in Fig. 3.

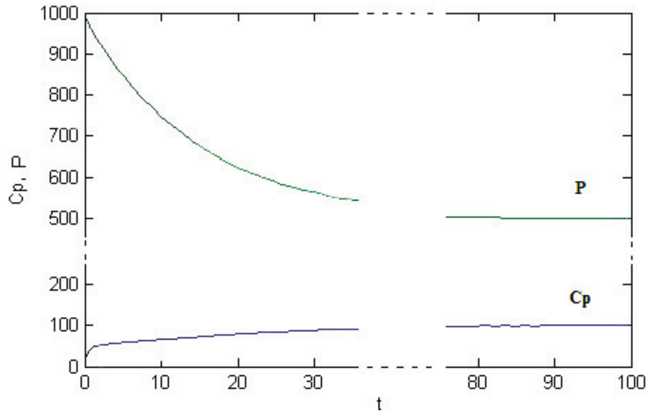

Fig. 3. Modeling of transition processes

Table 1. Parameters of dynamic model

Parameters	τ	η_B	γ	C_B	M	V	ΔB_P	β	ΔP	P_0	C_{P0}
Value	15	0.5	1 W/L	50 UAH/L	100000 UAH	1	0 L	1	0 W	1000 W	10 UAH/W

In the period of time $t = 0$ there is a decrease in the made power by 500 Wt, at the same time the tariff price increases according to a balance condition.

The resulting system allows calculating the dynamic defaults P and C_P after transient processes completed, when $\frac{dC_P}{dt}$ and $\frac{dP}{dt}$ are equal to zero.

From the first equation of (16), calculated relative C_P received:

$$C_P = \frac{M \cdot V - \Delta B \cdot C_B}{P + \beta \cdot P + \Delta P}. \tag{17}$$

From the second equation of (16), taking into account the expression for C_P obtained in (17), derived the following equation:

$$P^2 \cdot (-C_B - C_B \cdot \beta)$$

$$+ P \cdot (-\Delta P \cdot C_B + \eta_B \cdot \gamma \cdot \beta \cdot M \cdot V - \eta_B \cdot \gamma \cdot \beta \cdot \Delta B \cdot C_B)$$

$$+ \eta_B \cdot \gamma \cdot \Delta B = 0. \tag{18}$$

To solve a quadratic equation is performed substitution:

$$a = (-C_B - C_B \cdot \beta),$$

$$b = (-\Delta P \cdot C_B + \eta_B \cdot \gamma \cdot \beta \cdot M \cdot V - \eta_B \cdot \gamma \cdot \beta \cdot \Delta B \cdot C_B),$$

$$c = \eta_B \cdot \gamma \cdot \Delta B,$$

$$\sqrt{D} = \sqrt{b^2 - 4 \cdot a \cdot c}.$$

Since the money supply *M* is usually much higher than the value of other components of the equation (18), multiplier *b* will be positive. Accordingly, just one of the roots of the equation (18) will be positive: $P = (-b + \sqrt{D})/(2 \cdot a)$.

Substituting the resulting value P in the equation (17) and solving it, we will found expression of the tariff price: $C_P = (M \cdot V - \Delta B \cdot C_B)/(P + \beta \cdot P + \Delta P)$. With further research should be considered as a dynamic system parameters change and new static power value *P* and tariff price C_P, calculated in the steady state, after the transition.

6. CONCLUSIONS

It is offered static model of calculation of the price for various alternative sources. The developed algorithm of calculation of static price of electricity from alternative sources of the electric power for the consumer will allow the consumer to make reasoned decision on buy/sale the electric power. It is presented electro-cost model of the isolated power generating system allowing counting both dynamic change of the generated power, and dynamic change of the tariff price of the electric power taking into account static sizes of these parameters after completion of transition processes. Provided in paragraph IV dynamic model of isolated electro-cost system allows investigating changes in tariff price when the generator is switches to a new power regime. Using of the proposed electro-cost model of an isolated power generating system allows calculating the dynamic change of generating power and the dynamic change of the electricity tariff price, taking into account the static values of these parameters after the transition.

REFERENCES

[1] GREBENYUK G.G., SOLOVYOV M.N., *Continuous tariff regulation for the formation of the desired schedule download Power Systems*, Automation and Telemehanika, 2004, No. 6, pp. 166–169.

[2] ZHUIKOV V.J., PETERGERYA J.S., *Managing local power facilities on the basis of economic models*, Technical electrodynamics. Special issue of “Power Electronics and Energy Efficiency”, Part 2, 2000, pp. 131–136.

[3] ZHUIKOV V.J., PETERGERYA J.S., SADRYTSKYY R.V., *Managing energy consumption in the local cost objects using electrical models*, Technical electrodynamics. Special issue of "Power Electronics and Energy Efficiency", Part 4, 2003, pp. 49–53.
[4] ZHUIKOV V.J., PETERGERYA J.S., *The new concept of building control systems of electric power converters*, Technical Electrodynamics, 1998, No. 4, pp. 33–37.
[5] GERMEIER Y.B., *Game nonconflicting interests*, Publishing house "Science", Moscow 1976, 328 pp.
[6] INTRILIGATOR M., *Mathematical methods of optimization and economic theory Intriligator*, Trans. from English, Progress, Moscow 1975, 606 pp.
[7] KYRYLENKO O.V., PETERGERYA J.S., TERESCHENKO T.O., ZHUIKOV V.J., *Intelligent control system flows of electricity in local facilities*, Media Press, Kyiv 2005, 212 pp.
[8] KLEPACH L.E., *Managing power consumption on techno-economic parameters*. VIII International Scientific Conference of Young Scientists "Electronics-2015", 2015, pp. 227–231.
[9] MOROZ L.A., *Marketing: Textbook*, Intelekt. – West, Lviv 2002, 244 pp.
[10] NEUMARK Y.I., *Pricing model*. Proceedings of the universities, Applied Nonlinear Dynamics, 1996, No 6, pp. 35–42.
[11] PETERGERYA J.S., *Electro-cost models of generators and loads to control the power consumption of the local object*, Electronics and Communications, 2006, No. 2, pp. 33–39.
[12] PETERGERYA J.S., *Principles of intelligent control systems converters in local facilities*. Coll. works scientific conference "Ecotechnology and resursosberezhenie. Energy efficiency and protection of environment", pp. 17–21.
[13] PETERGERYA J.S., ZHUIKOV V.J., *Principles of effective intelligent energy management in local facilities*, Technical electrodynamics. Special issue of "Problems of modern electrical engineering", Part 1, 2002, pp. 90–96.
[14] USHAKOV D.R., *Of the value of the power for the guaranteed power supply*. VI International Scientific Conference of Young Scientists "Electronics-2013", 2013, pp. 319–322.
[15] HODAKOV V.E., SHERSTOK V.G., STEPANSKY K.G., DIDAK A.A., MARTYNOV A.M., *Methods of assessing the contradictory knowledge through relationship discord*, Electronics and Computer Science, 1998, No. 1, pp. 129–132.
[16] *European Smart Grids Technology Platform. Vision and Strategy for Europe's Electricity Networks of the Future*, Office for Official Publications of the European Communities, Luxembourg 2006.
[17] LEDIN S.V., *Koncepciya «elektrojenergija – tovar» kak katalizator razvitiya Smart Grid*, Avtomatizaciya v Promyshlennosti, 2012, 4, 4.
[18] BORDO M.D., *Equation of exchange*, The New Palgrave, *A Dictionary of Economics*, 1987, Vol. 2, pp. 175–177.
[19] POST D.L., COPPINGER S.S., SHEBLE G.B., *Application of Auctions as a Pricing Mechanizm for the Interchange of Electric Power*, IEEE Transactions on Power Systems, 1995, Vol. 10, No. 3 (August).
[20] ZHUIKOV V., PETERGERYA J., IVANIN O., *Electro-cost models of sources and loads for local object power control*, 10th International Workshop "Computational Problems of Electrical Engineering", At Waplewo, Poland, 2008, Vol. 3.
[21] ZHUIKOV V., PICHKALOV I., BOYKO I., BLINOV I., *Price formation in the energy markets of Ukraine*, Electronics and Nanotechnology (ELNANO) 2015, IEEE 35th International Conference, 2015.
[22] SHAHIDEHPOUR M., YAMIN H., LI Z., *Market Operations in Electric Power System*, Wiley, New York 2002.
[23] KORENEFF G., SEPPALA A., LEHTONEN M., KEKKONEN V., *Electricity spot price forecasting as a part of energy management in deregulated power market*, Energy Management and Power Delivery, 1998.

[24] ESMAEILI A.K., EGHLIMI M., OLOOMI M.B., SHAKOURI H.G., *Forecasting the electrical energy price in Iran power market: A comparison between single and multi-hour models*, IPEC, 2010 Conference Proceedings.
[25] DAVID A.K., Lee Y.C., *Dynamic tariffs: Theory of utility–consumer interaction*, IEEE Transactions on Power Systems, August 1989, Vol. 4, No. 3.
[26] TAYLOR J.A., NAYYAR A., CALLAWAY D.S., POOLLA K., *Consolidated Dynamic Pricing of Power System Regulation*, IEEE Transactions on Power Systems, Vol. 28, Iss. 4.
[27] XIAOHUI LIANG, XU LI, RONGXING LU, XIAODONG LIN, *UDP: Usage-Based Dynamic Pricing with Privacy Preservation for Smart Grid*, IEEE Transactions on Smart Grid, Vol. 4, Iss. 1.

bifurcation, feedback signal gain,
precision system, converter, chaos.

Valeri ZHUIKOV*
Andrii MATIIKO*

CHAOTIC PROCESSES IN PWM CONVERTER

The possibility of chaotic oscillations in them is determined. The structure of the chaotic oscillations in the DC converter is considered. The system stability at various gain values of the feedback signal is investigated. The task is building a precision DC buck converter. The goal is achieved by means of providing high feedback signal gain converter operation mode. The work of the converter is commended in a case of: a) changing the input voltage; b) changing the value of the load resistance. It is shown that while ensuring the appropriate converter operation mode it is possible to improve stabilising properties and reduce the system operation frequency.

1. INTRODUCTION

Chaos is largely unpredictable long-term evolution occurring in deterministic, nonlinear dynamical system because of sensitivity to initial conditions. Power electronics circuits are rich in nonlinear dynamics. Their operation is characterised by the cyclic switching of circuit topologies which gives rise to a variety of chaotic behaviour [1–3].

The first publications in scientific power electronics journals, which investigated issues related to the chaotic work regimes appeared in the 80s of the 20th century in the wake of interest in chaos and synergy. The most common bifurcations in power electronics are Hopf bifurcation (creation of a limit cycle), and the doubling of the period, which can be observed in other nonlinear systems. Besides that a special phenomenon can be observed in power electronics systems – border collision, related to the fact that due to the large velocity of the output parameter change it is possible to miss the commutation points and transition to lower subharmonics [4].

---

* National Technical University of Ukraine "Kiev Polytechnic Institute", Faculty of Electronics, Department of Industrial Electronics, 16, Polytechnichna str., off. 313, Kyiv, 03056, Ukraine, e-mail: amdrew.matiyko@gmail.com

There would seem to be two reasons for studying nonlinear dynamics in the context of power electronics:

- to understand better the nonlinear phenomena that occur in power converters, and thereby avoid undesirable effects,
- to allow converters to be engineered that deliberately make use of effects such as chaos.

Though the first objective has been achieved to some extent, there are yet few practical power electronics applications in which subharmonics or chaos bring a distinct advantage. Nevertheless, with increasing awareness among power electronics practitioners of nonlinear dynamics, perhaps engineering uses will soon be found for nonlinear effects. It may be helpful to list the characteristics of chaos, and indicate some possible application areas [5].

2. PWM CONVERTER MODEL

Processes occurring in the power part of the buck PWM DC (Fig. 1) converter are described by a system of equations:

$$\begin{cases} (di(t)/dt) = -(sr/L)i(t) - u(t)/L + sE/L, \\ du(t)/dt = i(t)/C - u(t)/RC, \end{cases} \tag{1}$$

and the processes in the feedback loop are described with the following system of equations:

$$\begin{cases} U_p = k(U_r - k_d U), \\ U_k = U_g - U_p, \\ s = s(U_k), \end{cases} \tag{2}$$

where E – the power supply voltage; L, C, R, r – linear inductance, capacitance, load resistance and the internal power supply resistance; $u(t)$, $i(t)$ – the capacitor voltage and the inductor current respectively; s – switching function, k_d – divider transfer coefficient, U_r – voltage reference element.

In accordance with the control system operation algorithm voltage U_p (the output voltage of the error signal amplifier) is compared in a comparator with voltage U_g ($U_g(t) = U_{ag}(t - nT)/T$, $n = 1, 2, 3, \ldots$; $0 \le t \le T$; U_{ag} – the amplitude voltage value of the scanning voltage ramp generator). On the comparator's output rectangular pulses that correspond to the intervals of the closed (switching function $s = 1$ for $U_k > 0$) and open ($s = 0$ for $0 \le U_k$) states of converter's power key are formed [3, 4].

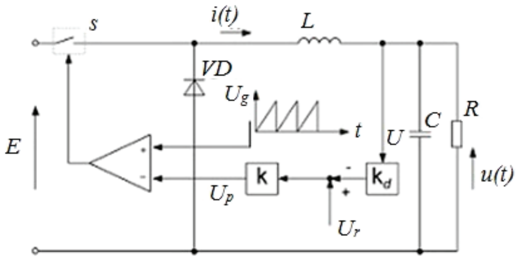

Fig. 1. PWM DC converter

3. CHAOTIC OSCILATIONS STRUCTURE

The structure of the chaotic oscillations varies depending on the gain value. With gradual increase of it system moves sequentially from steady state to chaotic processes and vice versa, forming zones of chaotic oscillations corresponding to a certain range of the coefficient *k*. For circuit parameters of buck converter: R = 100 Ohms; r = 0.1 Ohm, L = 0.1 H, $C = 10^{-6}$ F, E = 1000 V, U_r = 10 V, U_M = 10 V, T = 0.001 s, k_d = 0.01, the characteristic polynomial roots p_1, p_2 are valid (if $s = 0 - p_1 = -8873.0$, $p_2 = -1127.0$, while at $s = 1 - p_1 = -8872.8$, $p_2 = -1128.2$). Bifurcation diagram for time between the switching moments for the range of gain change k = 1 – 200 with increment Δk = 0,01 was built (Fig. 2). On this diagram, chaotic oscillations, which alternate with local zones of stability (ZS), are displayed [6].

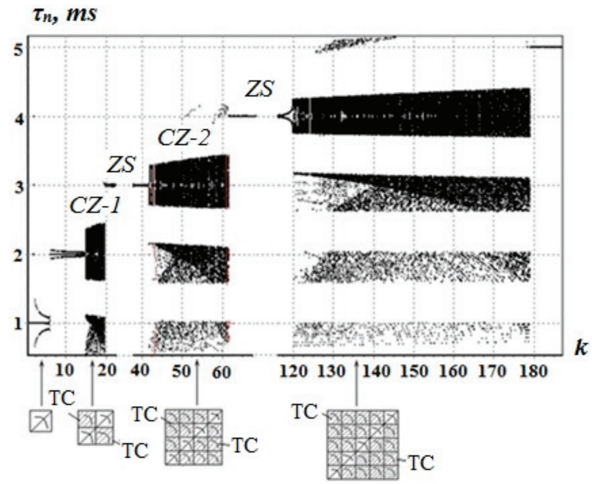

Fig. 2. Bifurcation diagram for time between the switching moments.
CZ – chaotic zone, ZS – zone of stability, TC – transfer curves for different chaotic zones

Figure 2 shows the chaotic zone CZ-2, CZ-3, which alternate with zones of stability (ZS) with a repetition period of 3T, 4T, 5T. Clusters of chaotic oscillations constitute the separate area of chaotic processes with relevant transfer curves (TC) [9]. Relation law between the number of homogeneous chaotic processes and the value of the gain is not linear. Thus, during the transition from the second chaotic zone (CZ-2) in the third (3-CZ) the number of homogeneous chaotic processes increased 2 times at 4, while the other parameters in [9], for a cluster following the CZ-2, the number of homogeneous random processes is equal to 3. The number of transfer curves of the corresponding map is also changed. With further increase of the gain (more than 400), a decrease in the number of homogeneous random processes from 8 to 4 with a decrease in the number of transfer curves is observed. This fact also indicates the existence of a non-linear relationship between the numbers of homogeneous random processes contained in the cluster to the gain of the feedback loop.

The mapping for the first zone and the resulting process is not different from the logistic map, and the corresponding process. A different situation is observed for the chaotic processes corresponding to zones CZ-2, CZ-3. Map, constructed in the usual manner, leads to an ambiguous map, as shown in Fig. 3, a. Otherwise, the map is obtained if after each bifurcation point, corresponding to the intersection of the reference voltage with the feedback signal, transfer origin for the start of the sweep voltage following the bifurcation point. In this case, the map takes the form shown in Fig. 3b, where on the central line there are maps for all homogeneous chaotic process for k = 50; and so-called TC, which provide a transition from one homogeneous process to another (over and under the central line) [8].

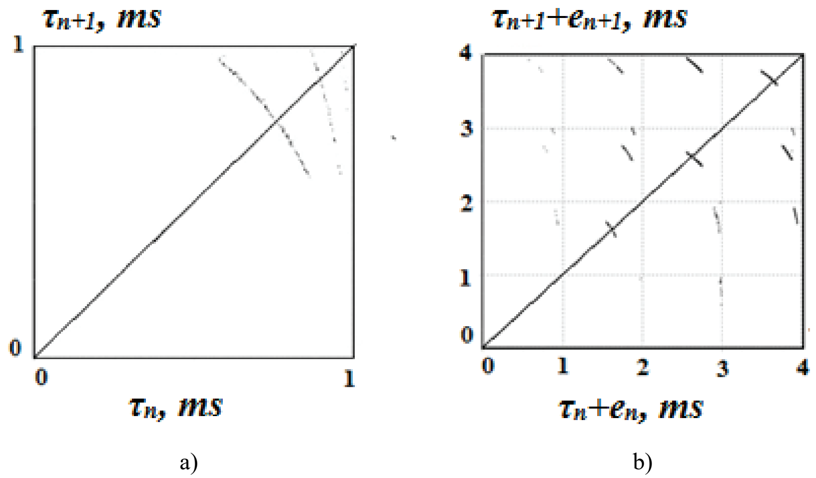

Fig. 3. Poincare map for k = 50

The nonlinear dependence of the sequence of numbers formed from the integral periods of the sweep voltage between moments of switching is preserved. For example, for the third chaotic zone CZ-3, with a gain $k = 50$, the formed sequence of integers, corresponding to the number of sweep voltage periods between moments of switching is given in Table 1 in a second row, where the first row indicates the number of switching moment.

Table 1. Sequence of switching moments

<table>
<tr><td>Switch moment number.</td><td>1</td><td>2</td><td>3</td><td>7</td><td>...</td><td>15</td><td>16</td><td>17</td></tr>
<tr><td>Sweep voltage periods number</td><td>3</td><td>2</td><td>2</td><td>2</td><td>...</td><td>2</td><td>2</td><td>2</td></tr>
<tr><td>Number of repetitions</td><td>1</td><td colspan="7">16</td></tr>
<tr><td colspan="9"></td></tr>
<tr><td>Switch moment number.</td><td>18</td><td>19</td><td>20</td><td>21</td><td>22</td><td>23</td><td>24</td><td>25</td></tr>
<tr><td>Sweep voltage periods number</td><td>1</td><td>1</td><td>2</td><td>2</td><td>1</td><td>1</td><td>1</td><td>1</td></tr>
<tr><td>Number of repetitions</td><td colspan="2">2</td><td colspan="2">2</td><td colspan="4">4</td></tr>
</table>

The third row of the table shows the number of repetitions of the amount of switching interval, that forms the second sequence that probably should also have a chaotic character [7]. The corresponding timing diagram is shown in Fig. 4.

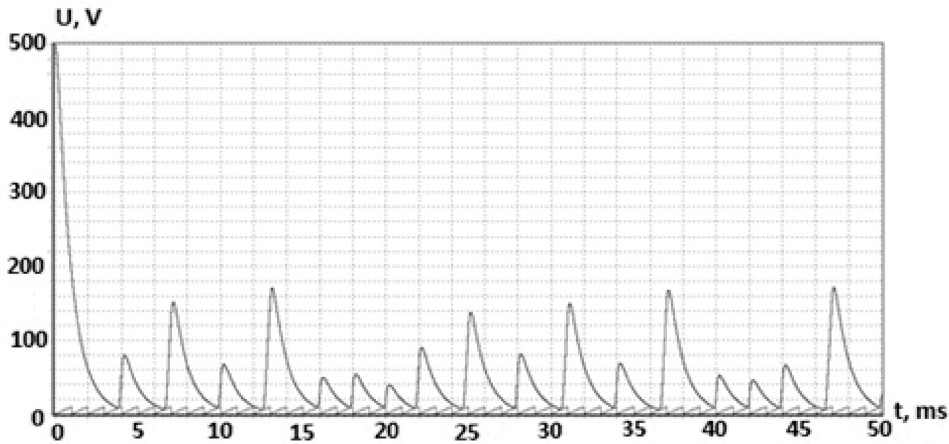

Fig. 4. Time diagram for $U_{zw}(t)$

4. SYSTEM STABILITY

Table 2 shows the characteristic equation roots values for different gain values.

Table 2. The characteristic equation roots values

Gain values	Characteristic equation roots values	
	*Z*1	*Z*2
6	0.5	0.9
15	–264	–14
20	0.26	–126.66
45	–0.65	–765.875
70	0.153	0.945
80	0.0175	–1163.07

Figure 5 schematically shows the characteristic equation roots location; as can be seen, in all cases, when the system is unstable, except for $k = 15$, one of the characteristic equation roots is in a unit circle, and root is shifted to the right with the gain value increase; second root with the gain value increase is shifted to the left. For both gain values at which the system is stable, both roots are in the right part of the unit circle.

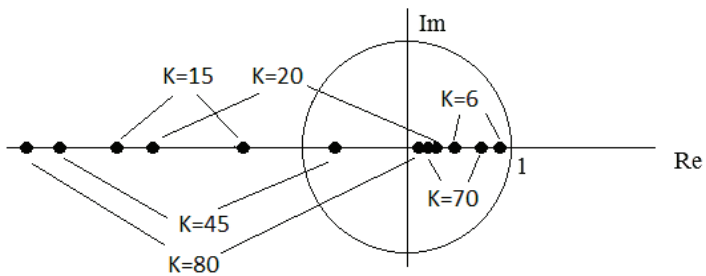

Fig. 5. The characteristic equation roots location

5. HIGH FEEDBACK SIGNAL GAIN PWM CONVERTER OPERATION MODE

Figure 6 shows a schematic representation of the bifurcation diagram, which was built gain increments $\Delta k = 0.01$ in the range of $k = 1 \div 90$; modelling is completed for 500 periods of scanning voltage for each value of k.

From Fig. 6 it can be seen that the 10% input voltage reduction causes the chaotic oscillations zone moves in the direction of the gain value reduction. When using high gain it is necessary to consider the position of the local zones of stability. With the big changes of the input voltage chaotic zone shifted so much that it cover the local zone of stability. Thus, it is possible to switch the converter to operate with the high gain, providing around 10% input voltage change.

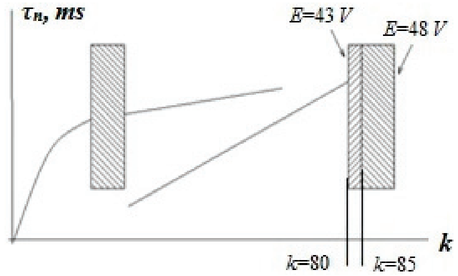

Fig. 6. Schematic representation of the bifurcation diagram

Figure 7 shows model's bifurcation diagram studied with R_1 = 4.8 Ohm, with relevant lines chaotic zones borders changes with 10% load resistance increasing (R_2 = 5.6 Ohm) and decreasing (R_3=4.3 Ohm) are shown. As it is shown in Fig. 7, with increasing of the load resistance value local zones of stability becomes wider (k = 23 ... 92), and with decreasing – becomes narrower (k = 26 ... 57).

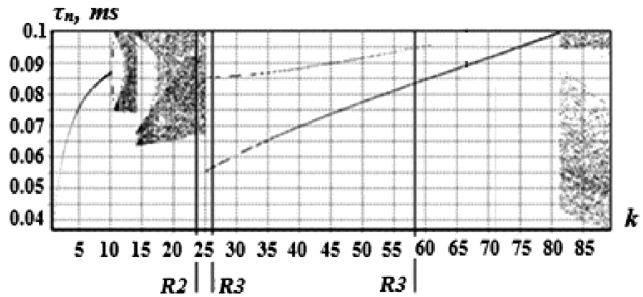

Fig. 7. Bifurcation diagram for different load values

Now the possible range of feedback signal gain can be determined. To ensure the stable operation mode of converting feedback signal gain should be in two bands.

The first range – from k = 1 to the start of the first chaotic zone. However, this option cannot provide necessary performance quality of converter.

The second range is located between the first and second chaotic zones and the feedback signal gain value must be in the range where switching occurs at a constant frequency. The critical value of gain is the beginning of the second chaotic zone for the converter with the load resistance R_3 = 4.3 Ohm.

Thus, to ensure the stable operation mode the feedback signal gain must be in the range of k = 67 ... 75. As the calculations for k = 70 showed, the load voltage ripple factor for the converter with the high feedback signal gain almost hasn't changed – $K_R = u_{max}(t)/u_{mid}(t)$ = 1.036 (with k = 6 K_R = 1.013), but the stabilisation rate has increased – $K_{ST} = (\Delta E/E)/(\Delta u(t)/u(t))$ = 22.25, while for k = 6 K_{ST} = 5.11.

The simulation results indicate that it is possible to build a precision system with the high feedback signal gain.

Figure 8 shows the voltage and current diagrams for $k = 70$. As it can be seen, switching frequency decreases 4 times from: 1) $f = 10$ kHz to 2) $f = 2500$ Hz.

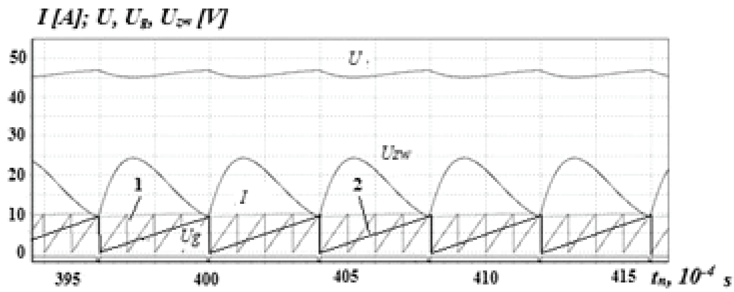

Fig. 8. Voltage and current diagrams for $k = 70$

As shown in Fig. 8, the reduced switching frequency did not change the output voltage, the frequency change also has not affected the voltage ripple factor and the stabilisation rate; roots-mentioned characteristics equation and the boundary of the converter vary slightly. Therefore, by increasing the feedback signal gain it is possible to reduce the switching frequency of the power key for reducing the switching losses in the system.

6. COCLUSIONS

The chaotic oscillations processes should not be described by differential equations of the less than second order. The equation order to boost converter circuit does not increase and chaotic oscillations in the steady state are not observed.

The cluster of chaotic oscillations does exist, but it is hard to specify how much homogeneous random processes it consists of and how much transfer curves mapping it contains because the cluster is described in more difficult conditions of existence. Relation law between the number of homogeneous chaotic processes and the value of the gain is not linear

Calculations show that it is advisable to ensure converter operation at a high feedback signal gain value to increase the stability and reliability of the system. In addition, the increasing of the feedback signal gain value may reduce the switching frequency of the system.

An ability of high feedback signal gain operation mode is shown. the load voltage ripple factor almost hasn't changed. However, as expected, the stabilisation rate has increased.

Also, by increasing the gain of the feedback signal may reduce the switching frequency and the frequency of the system, which reduces switching losses.

REFERENCES

[1] ADDISON P.S., *Fractals and Chaos. An illustrated course*, IOP Publishing Limited, 1997.
[2] HILBORN R.S., *Chaos and Nonlinear Dynamics*, An introduction for scientists and engineers, Oxford University Press, 1994.
[3] HAMILL D.C., BANERJEE S., VERGHESE G.C., *Introduction in Nonlinear Phenomena in Power Electronics*, ed. by S. Banerjee and G.C. Verghese, IEEE Press, 2001.
[4] DENISOV Yu.A., VELIGORCKIIJ A.A., *Modeling chaos in PWM DC voltage converter*.
[5] BANERJEE S., VERGHESE G.C., *Nonlinear phenomena in power electronics*, John Wiley & Sons, Hoboken, NJ, 2001.
[6] BRUSHKO V.V., ZHUYKOV V.Ya., *Randomization voltage regulator dynamics with PWM regulation*, Tehnicheskaya Elektrodinamika, Kiev, Ukraina, 1999, Silovaya elektronika i energoeffektivnost Ch. 3, pp. 115–118.
[7] BERZHE P., POMO I., VIDAL K., *Order in Chaos*, Mir, Moscow 1991, 367 pp. (in Russian).
[8] ZHUYKOV V.Ya., MATIIKO A.A., *The structure of chaotic processes in voltage converter*, Tekhnichna Elektrodinamika, Part 3, 2014.
[9] ZHUYKOV V.Ya., KOLICHENKO M.E., *Cluster of chaotic oscillations*, Tekhnichna Elektrodinamika, Part 3, 2013, pp. 29–33.

capacitor bank, power loss,
voltage profile, distribution system,
MATLAB

Sunny KATYARA*, Madad Ali SHAH*,
Jan IŻYKOWSKI**

POWER LOSS REDUCTION WITH OPTIMAL SIZE AND LOCATION OF CAPACITOR BANKS INSTALLED AT 132 kV GRID STATION QASIMABAD HYDERABAD

With growing concerns about voltage profile and power factor at distribution networks, the capacitor banks are invariably installed for reactive power compensation. The reactive power supplied by capacitor banks is proportional to square of their rated loading voltage. Capacitor banks eventually increase the loading capacity of feeders, so as to supply more customers through same line section. Capacitor banks can be installed anywhere on the network.

The idea of this paper is to reduce total power loss and ensure greater availability of capacitor bank installed at 132 kV grid station Qasimabad Hyderabad, for reactive power compensation, even under worst conditions on distribution system. This is achieved by enhancing its location and size. At present capacitor bank of full size, i.e. of 1.21 Mvar is installed at 11 kV bus of 132 kV grid station Qasimabad Hyderabad. Moreover this paper suggests small sized capacitor banks that would be installed at different feeders instead of one large size capacitor bank at 11 kV bus. The voltage profile and power losses with present sized capacitor bank and the proposed small sized capacitor banks are compared in this work. The distribution network has been simulated by using MATLAB Simulink.

1. INTRODUCTION

Modern power distribution systems experience rise in power losses during summer period [1]–[2]. This is mainly related to the excessive use of reactive loads. Such rise in this nature of load is supplemented with stumpy power factor (~78%) so it requires large reactive power transfer from the utility via network. The prime

* Sukkur Institute of Business Administration, Pakistan.
** Wrocław University of Science and Technology.

disadvantage of this issue is the rise of network losses and discount of voltage profile. Low voltage profile leads to malfunctioning or reduction in the lifetime of electric devices and increases the internal losses of cables and motors; hence decreases the efficiency [3]. For reactive power reparation, shunt capacitors are invariably installed at grid station. The main purpose of these capacitor banks is to lessen line and energy losses, sustain paramount voltage regulations at load buses and advance power network safety [4]. The extent of compensation delivered is highly associated to the location of capacitors in the utility network which fundamentally is the investigation of the position, size, numeral and sort of capacitors to be installed in the network [5]. A diverse range of investigation has already been performed on capacitor bank's placement and size problem in the past. But in this our research work we have presented a new technique for capacitor bank location and size so as to lessen total power loss to a greater extent.

Since power distribution network of 132 kV grid station Qasimabad Hyderabad has four transformers and 25 feeders, spreading geographically to supply major parts of Hyderabad city. The capacitor banks of 1.21 Mvar are invariably installed at four transformers buses for reactive power compensation of all feeders. The voltage levels of distribution feeders have greater voltage drop under the substantial load circumstances. Subsequently it offers unproductive facility to its users [6]. Procedures to resolve this issue are considering different techniques such as indigenous capacitor discrepancy, loss bargaining through capacitor installations, installation of synchronous generator, improvement through three phase balancing of utility system, constructing new substations, erecting new feeders and load balancing among feeders or incorporating photo voltaic production to distribution networks [7]–[8]. Capacitor bank position is the usual technique to decrease line losses and to sustain voltage profile beneath the restraints due to economy, modest connection and unpretentious apparatus [9].

However if a big size capacitor bank installed at 11 kV bus fails then regulation for whole feeder would be lost. Therefore proposed idea is to install small sized capacitor banks on each individual feeders. The size of this small sized capacitor bank would be calculated on the basis of reactive power demand of that particular feeder. With this arrangement not only total power loss reduces but also high availability of capacitor banks and accurate voltage regulation can be achieved. Means if any of capacitor bank at any feeder fails then it would not affect the regulation of other feeders as with the failure of large sized single bank installed at 11 kV bus. Although the cost of replacing large size capacitor bank installed at 11 kV bus by small sized capacitor banks installed at individual feeders is more [10] which is actually a disadvantage but mercy is that the transient produced by small sized capacitor banks are less than that of large sized capacitor banks. So the power loss contributed by these small sized capacitor banks would also be small. Therefore the money saved on these losses by small sized capacitor banks is approximately same as cumulative extra cost invested on these small sized capacitor banks for installation.

In this research work, investigative methods have been implemented to examine the capacitor bank's position and its size for decimation of total line losses and cost discount in utility feeders. Also if the location of capacitor is changed from bus with large capacitor bank to individual feeders with small sized capacitor banks then either the voltage profile of system is maintained or not. And also it has been analyzed that whether the system is balanced or unbalanced, it would not affect the system regulation if individual small banks are being installed at different feeders [11]. All these consequences have analyzed through MATLAB simulations.

2. DISTRIBUTION NETWORK CHARACTERISTICS

2.1. OBJECTIVE FUNCTION AND LINE LOSS ESTIMATION

Mathematically, an objective function is used to express the network's characteristics. It is used to minimize the power loss and deviation in the voltage [1]–[2]. This objective function is given by the expression (1):

$$F = W_1 P_{\text{loss}} + W_2 \sum_{n} (1 - V_i)^2 \tag{1}$$

where W_1 and W_2 are the coefficients of the objective function for the line power losses and voltage deviation, P_{loss} is the total power loss on the distribution network and V_i is the magnitude of the voltage on the i-th feeder.

The complex power at any bus, let say at the i-th bus, can be estimated by the expression (2):

$$P_k + jQ_k = V_k I_k \tag{2}$$

where P_k – real power of the k-th feeder, Q_k – reactive power of the k-th feeder, V_k – voltage at the k-th bus.

Gauss-Seidel iterative method can be used for calculating bus voltage and line losses by using the formula (3) [12]:

$$V_i(k+1) = \frac{1}{Y_{kk}} \left(\frac{P_i - jQ_i}{V_i(k)} - \sum_{n=1}^{m} Y_{in} V_n \right) \tag{3}$$

where $V_i(k)$ voltage at i-th bus after 1st iteration, P_k, Q_k – active and reactive powers at k-th bus, $Y_{m,n} = y_{m,n}$ with $m \neq n$ and $Y_{k,k} = y_{k,m-1} + y_{k,m+1} + y_{ji}$ with $m = n$.

In the line section the power loss between the buses i and $i + 1$, at the power frequency can be calculated by equation (4) [12]:

$$P_{\text{loss}}(i,i+1) = R_{i,i+1}\left[\left|V_{i-1} - V_i\right| \cdot \left|y_{i,i-1}\right|\right]^2 \tag{4}$$

where $Y_{m,i+1} = \dfrac{1}{R_{i,i+1} + jX_{i,i+1}}$ – admittance of the line section between buses $i + 1$ and m, $R_{i,i+1}$ – line connection bus resistance i and i+ 1, $X_{i,i+1}$ – line connection bus reactance i and i + 1.

The total power loss then can be calculated by using equation (5):

$$P_{\text{loss}} = \sum P_{\text{loss}}(i,i+1) \tag{5}$$

3. NETWORK REPRESENTATION

Figure 1 represents the 132 kV network of Qasimabad grid station Hyderabad which is consisting of two 132 kV lines, one is coming from Halla and other from Jamshoro. The 132 kV voltages are stepped down to 11 kV voltages at grid station by means of four Transformers, one of the transformer is rated at 40 MVA and other three are of 26 MVA. It is then distributed to Hyderabad city through 25 feeders. The 11 kV voltage of the feeder is actually its RMS value, the results calculated below are based on peak value which would be (11 kV * √2 = 15.554 kV). When there is heavy load on feeders then a considerable drop of voltage would be observed. For improving the voltage of system, the capacitor banks are installed at the buses before the feeders as shown in Fig. 1.

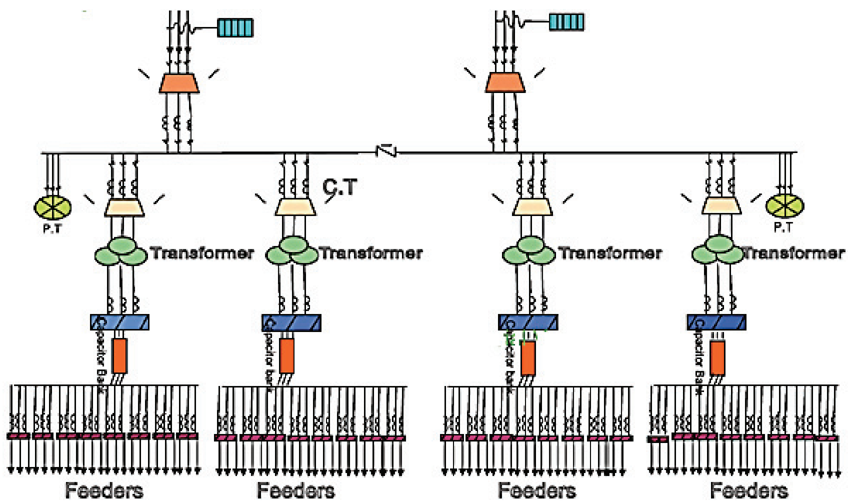

Fig. 1. Graphical illustration of 132 kV grid station Qasimabad, Hyderabad

4. POWER SYSTEM SIMULINK REPRESENTATION

Figure 2 presents the Simulink model of 132 kV grid station Qasimabad Hyderabad. The system was simulated with load of 10 MVA at a 0.87 lagging power factor. These standards were comprised in our MATLAB/SIMULINK model along with line inductances, capacitances, and resistances. The most significant components linked to the buses at the grid station is the static capacitor banks of 1.21 Mvar.

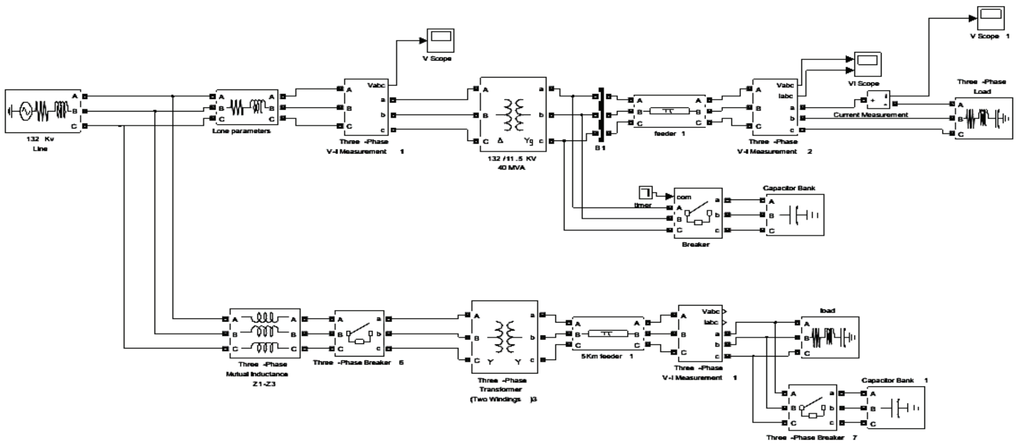

Fig. 2. Simulink model of 132 kV Qasimabad, Hyderabad grid station

5. RESULTS AND DISCISSION

The capacitors banks are normally installed at the buses on the grid station because the numbers of feeders which carry the actual load are connected to them. If we install a large capacitor bank at the bus in order to improve the voltage profile then the feeders which have normal rated loads will get shoot up in their voltages and may cause damage to associated equipments. Capacitors are always designed for largest length of feeders so as to maintain voltage at the far end of it. Since the reactive power supplied by the capacitor is proportional to square of its voltage. When the system voltage is down then reactive power supplied by capacitor will also be low and it is not useful because when we need reactive power then at instant it is not available. It is more convenient to install a separate capacitor bank of small size at each feeder, so that voltage profile could be corrected to the condition of that feeder and unnecessary drop should be avoided [14]. With this configuration the reliability system also increases because if any one of the bank is out of order then it will not influence other neighbouring lines.

5.1. BASE CASE

Initially when no capacitor bank was connected to 0 the system at 132 kV grid station Qasimabad Hyderabad, the system voltage was below the reference value *i*-e 15.554 kV (11 kV RMS) down to 14.14 kV (10 kV RMS) due to reactive power requirement as shown in Fig. 3.

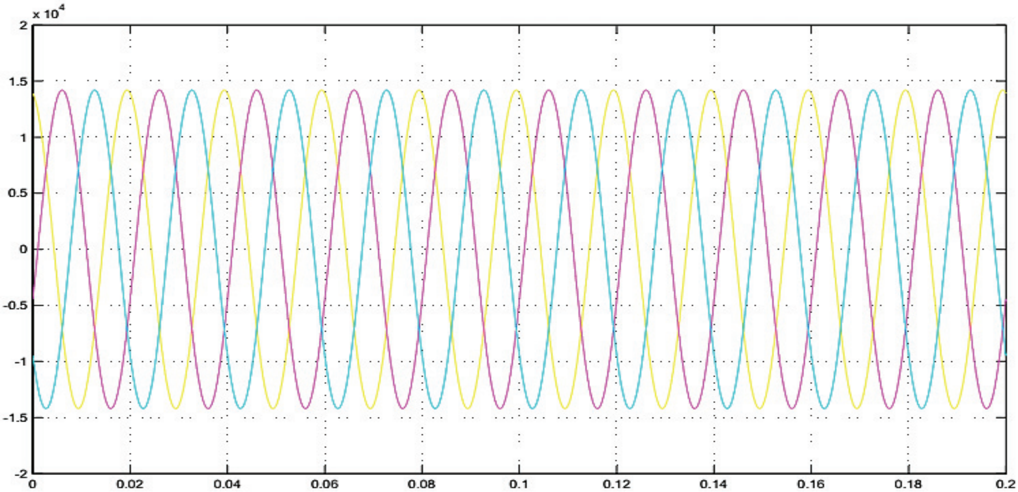

Fig. 3. Voltage at distribution network when no capacitor bank in service

5.2. CAPACITOR BANK (1.21 Mvar) IN SERVICE AT BUS

The size of star connected capacitor bank installed at grid station for reactive power is usually calculated by:

$$\text{Reactive Power} = \frac{V^2}{X_{\text{COMPENSATION}}} \tag{6}$$

Taking $X_{\text{COMPENSATION}} = 100\ \Omega$ would result in Reactive Power = $(11 * 1000)^2/100$ = 1.21 Mvar. When the capacitor banks of 1.21 Mvar were connected to 11 kV buses before the feeders, the voltage was increased from 14.14 kV (10 kV RMS) to 15.554 kV (11 kV RMS) and consequently high frequency transients were also produced at 0.08 sec of supply voltage frequency as shown in Fig. 4. These high frequency transients caused greater power loss in the system. Since now if any of the bank is out of order then, all the feeders connected to bus would lose their voltage regulation. Since the reactive power supplied by capacitor bank is proportional to square of its voltage, so if bus voltage dips below natural line value then power supplied by capacitor banks would reduce four times and it would be unavailable when needed the most.

Therefore it became necessary to install individual small sized capacitor banks at each feeder according to its own reactive power demand. Since the load on each feeder is not same, so the different voltage regulation would be needed for all individuals.

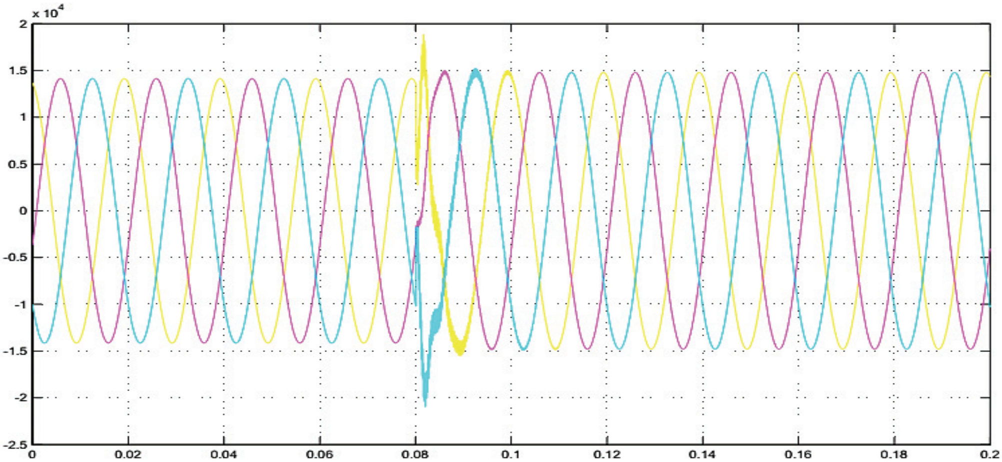

Fig. 4. Voltage at distribution network when capacitors bank is in service

5.3. PROPOSED SMALL CAPACITOR BANK IN SERVICE AT FEEDER

Our suggested way for calculating reactive power of small sized capacitor banks which would be installed individually at feeders is:

$$Q_{\text{bank}} = S_{\text{load}}(p.f_{\text{required}} - p.f_{\text{load}}) \tag{7}$$

Taking: $S_{\text{load}} = 3$ MVA, p.f.$_{\text{load}} = 0.87$, p.f.$_{\text{required}} = 0.953$ one gets: $Q_{\text{bank}} = 250$ kvar.

When capacitor bank of 250 kvar is connected across the Defence feeder installed at 132 kV grid station Qasimabad having load of 3 MVA with a power factor of 0.87 then its voltage improved to exactly 15.554 kV (11 kV RMS*)* and power factor was corrected to 0.953 as shown in Fig. 5.

Since from our above Table 1 it is proved that we can replace large sized capacitor bank having cost of US $ 8000/unit installed at 11 kV bus of 132 kV grid station Qasimabad Hyderabad at by small sized capacitor banks installed at individual feeders with approximately same price as whole of US $ 900/unit and same performance. Yes it is clear that somewhat cost is high, like for six different feeders on single bus the cumulative cost of all small sized capacitor banks would be: Cost = 900 * 6 = $ 5400, which is greater than $ 4000 for single 1.21 Mvar. Since the price of replacing banks for small sized capacitor is surely greater but the amount of money saved on loss reduction is much more than to it, because this replacement expenditure is just for once, then after saving would be for whole life of capacitor banks. The biggest advantage is that high availability of capacitor bank would have been achieved with this arrangement.

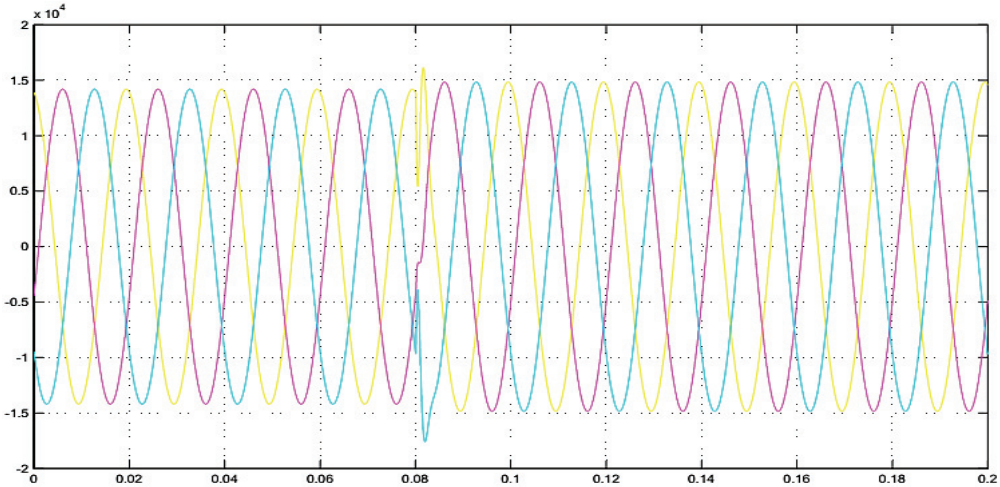

Fig. 5. Voltage at distribution network when small capacitor banks are in service

Table 1. Different companies' capacitor banks with their size and price

S. No.	Name of Brand	Rated Voltage	Rated Power	Price Per Unit
1	TK	11 kV	1.21 Mvar	US $ 4000
2	Daelim	11 kV	1.11 kvar	US $ 7200
3	HV shunt capacitor	1 kV~20 kV	50–800 kvar	US $ 5000–1800000
4	HOMOR	11 kV	100–10 000 kvar	US $ 900
5	ZHIYUE	11 kV	30–334 kvar	US $ 50–450
6	JCKN	11 kV	250 kvar	US $ 100–1000
7	ONLYSTAR	6.3–12 kV	50–500 kvar	US $ 200–2000
8	WIRUN	300 V–12000 V	100–500 kvar	US $ 20–1500

Table 2 shows the characteristic of Defence feeder with old installed capacitor bank and new proposed capacitor bank. It is perceived that total line loss for the utility feeder is 185564 W and loss discount is 12.364% with installed capacitor bank of 1.21 Mvar. But with the proposed capacitor bank the total power loss reduces to

169892 W and loss reduction comes to 12.982%. It is therefore less than total power loss of system. The cost per kvar is also less than that of installed bank. All these results are being calculated and generated by using equations (3), (4) and (5), which are stated above and results are being verified by means of simulations shown above. Thus proposed method offers more accurate reactive power compensation and more loss decimation for a utility feeder.

Table 2. Comparative analysis between installed and proposed capacitor banks

Particulars	Without Capacitor Bank	With Capacitor Bank	
		1.21 Mvar	250 kvar
Maximum Voltage in kV	10.76	11	11.03
Minimum Voltage in kV	10	10.87	10.98
Total loss in (kW)	191.431	185.564	169.892
Cost/kvar $	0.512	0.353	0.312
Loss reduction (%)	0	12.364	12.982

The proposed method offers more accurate reactive power compensation, effective loss reduction and perfect balance of voltage profile for each distribution feeder. This idea was implemented over all 25 feeders and resulting characteristics were illustrated in Table 3. It shows the loading ability of different feeders and on this basis size of capacitor bank was evaluated. With this proposed bank, the associated percentage loss reduction and limit of voltage profile for all 25 feeders is shown in Table 3.

Table 3. Characteristics analysis of different feeders at 132 kV grid station Qasimabad Hyderabad

Sr. No.	Load of Feeder (MVA)	Proposed Capacitor Bank Size (kvar)	Power Loss Reduction (%)	Voltage Profile (p.u.)
1	2	3	4	5
1	4.5	375	12.657	1.003
2	2.8	235	12.432	1.002
3	1.5	125	11.987	1.007
4	3	250	12.982	1.006
5	0.55	46	12.232	1.008
6	0.88	75	12.752	1.005
7	3.85	320	11.879	1.004
8	0.44	38	12.675	1.005
9	1.76	150	12.314	1.008
10	0.99	85	13.123	1.006
11	1.65	140	12.573	1.000
12	1.76	148	12.773	1.001

1	2	3	4	5
13	0.11	10	12.586	1.002
14	2.09	175	11.921	1.000
15	0.11	10	13.142	1.003
16	2.09	175	12.148	1.006
17	1.1	95	12.865	1.009
18	1.32	110	12.554	1.000
19	0.99	85	12.813	1.003
20	1.43	120	11.971	1.005
21	1.43	120	12.745	1.002
22	1.1	95	12.963	1.005
23	1.87	160	12.461	1.007
24	0.88	75	11.978	1.004
25	0.11	10	12.785	1.003

6. CONCLUSION

Since the enhancement of voltage profile, the reduction of line losses and their prices at 132 kV grid station Qasimabad Hyderabad were discussed in this research work by augmenting the size and location of the capacitor bank. It was analysed and calculated that installed capacitor banks of 1.21 Mvar at 132 kV grid station Qasimabad Hyderabad should be replaced with small sized bank of about 250 kvar calculated according to feeder load, which is different for different feeders. This proposed bank is to be installed at individual feeders, so that regulation characteristics on each it can be obtained precisely according to its reactive power demand. This technique also facilitates the high availability of capacitor banks which should be met during the peak load hours. Also with small sized capacitor banks less amplitude and low frequency transients would be produced, so the power losses in the system were found to be least. The cost of small sized capacitor banks with the sum to approximate the large sized single capacitor bank was high but the loss reduction and function of high availability obtained through the small sized capacitor banks were more outstanding than that of cost difference. It is therefore can be concluded that the results from suggested technique were preeminent; which guarantees the dominance of this proposed effort.

7. FUTURE RECOMMENDATIONS

Practical implementation of the capacitor bank placement technique requires further cost benefit analysis which in turn depends upon cost of capacitor bank and energy saving. Also the repeated simulation results could be used to develop a model using any artificial intelligence technique. This technique can accurately predict the location and size of capacitor bank for any load conditions without making any delay. It gives the great edge to implement our proposed technique practically.

ACKNOWLEDGEMENT

Associated authors are gratified to Mehran University of Engineering and Technology Jamshoro Pakistan for supporting our research work and providing free hand access to their laboratories. Authors are also thankful to technical staff of 132 kV grid station Qasimabad Hyderabad for helping to get required data. First author is very much thankful to Prof. Dr. Ashfaque Ahmed Hashmani and Prof. Dr. Bhawani Shankar Chowdhary for supporting and motivating our research work.

REFERENCES

[1] MILLER T.J, *Reactive power control in electric system*, John Wiley & Sons, Inc., New York 1982.
[2] BARAN M.E., WU F.F, *Optimal capacitor placement on radial distribution system*, IEEE Transaction on Power Delivery, Vol. 4, No. 1, January 1989, 725–734.
[3] CHEN C.S., SHU C.T., YAN Y.H., *Optimal distribution feeder capacitor placement considering mutual coupling effect of conductors*, IEEE Transactions on Power Delivery, Vol. 10, No. 2, April 1995, 987–994.
[4] GONEN T., *Electric power distribution system engineering*, McGraw-Hill, 1986.
[5] AL-HINAI S., ELLITHY K., AL-BADI A., AL-NOFLI A., AL-HATMI S., *Determination of optimal rating and location of shunt Var compensation for SQU distribution network*, Proceeding of GCC Cigré 13th Annual Seminar, Muscat, Oman, October 2002, 205–212.
[6] COELHO DE CASTRO C.L.C., DA SILVA M.G., RODRIGUES A.B., *Inclusion of voltage drop and feeder loading constraints in the evaluation of reliability indices for radial distribution networks*, Generation, Transmission and Distribution, IEE Proceedings, Vol. 4, No. 6, November 2006, 661–669.
[7] HAMADA M.M., WAHAB A., EL-SAYED M., RAMADAN A., *A proposed strategy for capacitor allocation in radial distribution feeders*, Power Systems Conference Proceedings, Vol. 4, No. 5, March 2006, 146–151.
[8] KYU-HO KIM, SEOK-KU YOU, *Voltage profile improvement by capacitor placement and control in unbalanced distribution systems using GA*, IEEE Power Engineering Society Summer Meeting, Vol. 2, No. 4, July 1999, 800–805.
[9] HSIAO-DONG CHIANG, JIN-CHENG WANG, JIANZHONG TONG, DARLING G., *Optimal capacitor placement, replacement and control in large-scale unbalanced distribution systems: system solution algorithm and numerical studies*, IEEE Transactions on Power Systems, Vol. 10, No. 1, February 1995, 363–369.
[10] NG H.N., SALAMA M.M.A., CHIKHANI A.Y., *Capacitor allocation by approximate reasoning fuzzy capacitor placement*, IEEE Transaction on Power Delivery, Vol. 15, No.1, January 2000, 393–397.

[11] KHODR H.M., ZERPA I.J., DE OLIVEIRA-DE JESUS P.M., MATOS M.A., *Optimal phase balancing in distribution system using mixed-integer linear programming*, Transmission and Distribution Conference Proceedings, August 2006, 1–5.
[12] MALANGE F.C.V., ALVES D.A., DA SILVA L.C.P., CASTRO C.A., DA COSTA G.R.M., *Real power losses reduction and loading margin improvement via continuation method*, IEEE Transactions on Power Systems, Vol. 19, No. 5, August 2004, 1690–1692.
[13] CHANDRA A., AGARWAL T., *Capacitor bank designing for power factor improvement*, ISSN 2250-2459, ISO 9001:2008 Certified Journal, Vol. 4, Iss. 8, August 2014.
[14] NATRAJAN R., *Power system capacitors*, Taylor & Francis Group, LLC, International Standard Book Number-I 0:1-57444-710-6, USA, May 1996, 45–67.
[15] MUHUMMAD A., MASOUM S., LADJEVARDI M., JAFARIAN A., FUCHS E., *Optimal placement, replacement and sizing of capacitor banks in distorted distribution networks by genetic algorithms*, IEEE Transactions on Power Delivery, Vol. 19, No. 4, October 2004, 1794–1801.